Economic Geology
Vol. 88, 1993, pp. 622–646

$^{40}Ar/^{39}Ar$, K/Ar, and Fission Track Geochronology of Sediment-Hosted Disseminated Gold Deposits at Post-Betze, Carlin Trend, Northeastern Nevada

G. B. AREHART,*

Department of Geological Sciences, University of Michigan, Ann Arbor, Michigan 48109-1063

K. A. FOLAND,

Department of Geological Sciences, Ohio State University, Columbus, Ohio 43210

C. W. NAESER,

U. S. Geological Survey, Mail Stop 484, Denver Federal Center, Denver, Colorado 80225

AND S. E. KESLER

Department of Geological Sciences, University of Michigan, Ann Arbor, Michigan 48109-1063

Abstract

The Post-Betze deposit of Nevada is the largest sediment-hosted disseminated gold deposit presently known, both dimensionally and in terms of contained metal. Ore occurs primarily as submicron-sized gold that is disseminated in altered sedimentary rocks of the Lower Paleozoic Roberts Mountains Formation. However, significant portions of the ore are present in altered monzonite of the Goldstrike stock. Alteration and mineralization were controlled by both structure and stratigraphy. Alteration began with early decarbonatization and was followed by silicification and, finally, argillization. Phyllosilicate mineral zoning grades from proximal kaolinite to kaolinite + sericite to unaltered rock.

Based on geochronologic studies utilizing the K/Ar, $^{40}Ar/^{39}Ar$, and fission track techniques, we suggest that the age of gold mineralization is approximately 117 Ma. The premineralization Goldstrike stock was emplaced at about 158 Ma and a postmineralization sill was emplaced at 39 Ma; these events place clear limits on the age of mineralization. Fine-grained sericite that is interpreted to have formed during hydrothermal events which also generated gold ore was dated by either the K/Ar method or a modification of the standard $^{40}Ar/^{39}Ar$ fusion technique. Age determinations on several samples of fine-grained sericite from altered host rocks (both sedimentary and igneous) yield ages near 117 Ma. Younger dates are interpreted to be the result of either thermal disturbance of the K/Ar system or mixing of sericites of two ages. One sample of coarser grained sericite that was stepheated gave discordant spectra.

Fission track analyses of zircon and apatite from the postore sill clearly document the lack of significant thermal or hydrothermal activity younger than 39 Ma. Although less definitive, fission track data on zircon from preore sedimentary and igneous hosts suggest that no widespread hydrothermal activity having temperatures above about 100°C has occurred since approximately 110 Ma.

The 117 Ma age is consistent with one of the major magmatic pulses recognized in the northern Great Basin. It is also similar to, within analytic uncertainty, a K/Ar date of 109 Ma from the Welches Canyon stock (20 km south of Post-Betze). An intrusion of similar age, unexposed at present, could have been the driving force for the hydrothermal system at Post-Betze.

Published geochronologic data, though less well tied to mineralization, suggest similar mid-Cretaceous ages for other sediment-hosted disseminated gold deposits in Nevada. Based on these ages, we suggest that sediment-hosted disseminated gold deposits are not necessarily products of extensional environments and, in fact, appear to be associated with compressional environments in Nevada during Cretaceous time. The alignment of sediment-hosted disseminated gold deposits (and other features) in the Basin and Range province of the west-

* Present address: Geosciences/CMT-205, Argonne National Laboratory, Argonne, Illinois 604389.

0361-0128/93/1447/622-25$4.00

ern United States suggests that zones of long-term crustal weakness may have controlled igneous intrusion and consequent hydrothermal gold mineralization, although not all igneous episodes necessarily generated sediment-hosted disseminated gold ore deposits. The strong association between sediment-hosted disseminated gold deposits, the Precambrian craton, and these deep-seated structures also suggests the possibility of a deep source for gold and other components of these systems.

Introduction

SEDIMENT-hosted disseminated gold deposits (also commonly known as "Carlin-type" deposits) comprise extremely fine grained disseminations of gold hosted by altered silty carbonate rocks. They are characterized by high Au/Ag ratios; a geochemical association of Au, As, Sb, Hg, and sometimes Tl and Ba; and a notable absence of base metal sulfides. The most conspicuous alteration features are the presence of highly silicified zones, commonly known as jasperoids, and decarbonatization of the host rocks (Bagby and Berger, 1985; Tooker, 1985). Although high-grade portions of these deposits, such as at Getchell and Mercur, have been mined sporadically since the last century (Joralemon, 1951; Kornze, 1984), they were not recognized as a distinct class of ore deposit until the discovery and development of Carlin and Cortez as bulk-tonnage mines in the mid-1960s (Hausen and Kerr, 1968; Wells et al., 1969). Sediment-hosted disseminated gold deposits did not become economically important until the mid-1970s, after the price of gold was freed from government price restrictions and allowed to rise to free market values. Since that time, sediment-hosted disseminated gold deposits have become a major source of gold in the United States.

Early research on sediment-hosted disseminated gold deposits consisted primarily of the development of geochemical exploration techniques and metallurgical extraction processes. Research into the origins of the deposits was frustrated by the scale of features necessary to elucidate origins and by the lack of good exposure of unweathered ore. It has been only because of the discovery of unweathered ores of economic interest and recent developments in analytical capabilities that some of the complexities of these deposits are being unraveled, producing a better understanding of their origin.

One of the major questions regarding sediment-hosted disseminated gold deposits is their age. An assortment of ages has been postulated for these deposits, based on a variety of lines of reasoning. A regional study of altered shales and illite veins led Wilson and Parry (1990) to suggest that Mercur is Mesozoic in age. A Cretaceous age is espoused by a variety of workers based on K/Ar dates on alteration minerals thought to be related to gold mineralization (Silberman and McKee, 1971; Silberman et al., 1974; Berger and Taylor, 1980; Bonham, 1985; Osterberg, 1990). Because most of the known deposits are located in the Great Basin, which experienced abundant igneous and hydrothermal activity through Tertiary time, others have concluded that sediment-hosted disseminated gold deposits are of Tertiary age (Joralemon, 1951; Wells et al., 1969; Radtke, 1985; Rota and Hausen, 1991). A pre-late Tertiary age was suggested by Bakken and Einaudi (1986) based on structural evidence in the Carlin mine. A number of jasperoid-hosted gold deposits are indirectly dated by Seedorff (1991) as mid-Tertiary. He proposed a model that required regional crustal heating of suitable source rocks combined with development of the appropriate "plumbing" for migration of hydrothermal fluids. These conditions are considered by him to have existed in early Eocene-Oligocene times, and he infers that age for other sediment-hosted disseminated gold deposits. Miocene or younger ages were suggested by Radtke (1985), from igneous rocks thought to be the possible heat source for the Carlin deposit; Birak (1986), from an absence of drop in ore grades across faults of Miocene age at Jerritt Canyon; and Ilchik (1990), from K/Ar dates on alunite at Alligator Ridge. Unfortunately, none of these ages have been determined on minerals or events that convincingly can be shown to have been related to the ore-forming event(s).

The Post-Betze Deposit

The Post-Betze deposit, which is located in the Carlin trend (Fig. 1), is the largest known sediment-hosted disseminated gold deposit, containing in excess of 25 M oz of reported gold reserves. Near-surface gold mineralization was known above this deposit as early as 1963, and several small surficial deposits were mined between 1975 and 1986 by Western States Mining. In 1982, the Post deposit was discovered by drilling to depths of 100 to 170 m, and by 1986 reserves were 11 million metric tons at a grade of 1.7 g/t Au (Bettles, 1989). The initial discovery of deep (>300 m) high-grade mineralization took place in late 1986, when drill hole 118 intersected a 120-m interval of mineralization averaging 6.0 g/t Au. The Goldstrike mine (which comprised largely the Post deposit but included several other small deposits) was sold in January 1987 to American Barrick Resources, which became the sole operator under the name Barrick Goldstrike Mines. Further deep drilling delineated a large sulfide gold orebody at depths of between 400 and 600 m, which was named Lower Post for its position beneath the original Post

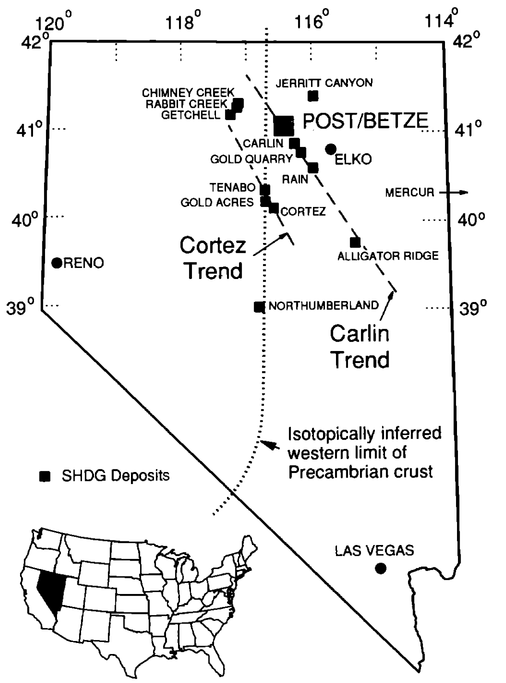

FIG. 1. Location map showing major sediment-hosted micron gold deposits of Nevada (deposits updated from Bonham, 1986, for new discoveries).

deposit. Based on geophysical, geochemical, and geological data, an exploratory deep drill hole was begun in early 1987, 1 km northwest of the Lower Post deposit; this drill hole intercepted 91 m of 12.7 g/t Au in two zones at depths between 250 and 450 m and was labeled the Betze deposit (Bettles, 1989). Subsequent drilling between these two deposits has shown that they are part of a large single orebody, which is herein called the Post-Betze deposit.

Our research focused on Post-Betze because it is the only deposit hosted in a significant part by igneous rocks, which we hoped would facilitate our dating efforts, and because the vertical extent of mineralized rocks at Post-Betze is much greater than at any other deposit known at present, allowing a more complete examination of alteration and mineral zoning in a sediment-hosted disseminated gold deposit and consequently a better selection of samples suited to dating. A major effort was initiated specifically to define the age of the Post-Betze deposit. Previous attempts to date sediment-hosted disseminated gold deposits by radiometric methods generally have been ancillary to other goals and generally consist of only one or two K/Ar dates on a single phase.

Regional Geology

The tectonic evolution of the Great Basin since the Late Proterozoic can be subdivided into three phases (Levy and Christie-Blick, 1989). The Late Proterozoic to Late Devonian times were characterized by intracontinental extension and development of a passive margin and associated sedimentation. From the Late Devonian to early Eocene, the region was in a compressional regime, which included accretion of exotic terranes and subduction-related magmatism. Since about 40 Ma, the region has been subject to lithospheric extension and associated magmatism.

The Carlin trend lies astride a major isotopic boundary inferred to be the western limit of Precambrian crust (Fig. 1). Initial $^{87}Sr/^{86}Sr$, ϵ_{Nd}, lead isotope, and whole-rock oxygen isotope values change markedly across this boundary (Zartman, 1974; Kistler and Peterman, 1978; Farmer and DePaolo, 1983; Solomon and Taylor, 1989). During early to middle Paleozoic time, the margin of the craton was an area of transition between deposition of shelf facies rocks to the east and deeper water, cherty facies rocks to the west (Stewart, 1980; Elison et al., 1990).

The oldest exposed units in the area are lower Paleozoic miogeoclinical sedimentary rocks of the Hamburg Dolomite, Pogonip Group, Eureka Quartzite, and Hanson Creek Formation (Table 1; Evans, 1980). Conformably above the Hanson Creek is the Roberts Mountains Formation, composed of dark gray fine-grained silty to sandy dolomitic limestone. This interfingers with the overlying Popovich Formation which was defined by Evans (1980) as the lowest thick-bedded intraformational breccia. Bakken and Einaudi (1986) designated these two lithologies as laminated silty limestone and massive fossiliferous limestone, respectively; the two types responded differently to hydrothermal fluids.

Overlying this miogeoclinical sequence is a cherty sequence that formed in deep water, and which is generally interpreted as time-equivalent rocks that originally were deposited to the west. These rocks have been informally termed the Rodeo Creek formation (Zimmerman et al., 1987), although they are considered to be part of the Vinini Formation by others (e.g., Radtke, 1985). The western sequence is interpreted as having been thrust eastward over the shelf facies along the Roberts Mountains thrust during the Late Devonian Antler orogeny (Roberts, 1960; Speed, 1979). Zimmerman et al. (1987), however, suggested that at least some structures previously interpreted as thrusts may instead be depositional features associated with primary turbidite and debris flow sedimentation, at least in the area of the Carlin trend. The present exposure of the Roberts Mountains thrust roughly follows the inferred craton margin where the western assemblage rocks were thrust onto the craton and subsequently eroded. In either case, this stratigraphic and/or structural sequence had been established prior to the Post-Betze mineralization.

These lower Paleozoic rocks, particularly the lami-

TABLE 1. Description of the Stratigraphic Section in the Vicinity of the Post-Betze Deposit (modified from Evans, 1980)

Rock unit	Age	Thickness (m)	Description
Rodeo Creek Formation	Devonian	>2,500	Interbedded dark gray to black, thin cherty shales and shaly cherts; minor amounts of interbedded massive limestone, argillite, and sandstone (probably includes the transitional assemblage limestone and some rocks of the Vinini Formation; Evans, 1980)
		Roberts Mountains thrust?	
Popovich Formation	Devonian	425	Thick to thin lenses of intraformational breccia that grade laterally into fine-grained limestone with abundant clastic debris, interspersed with laminated limestones similar to those found in the Roberts Mountains Formation; Bakken and Einaudi (1986) designated these two lithologies as laminated silty limestone and massive fossiliferous limestone
Roberts Mountains Formation	Devonian-Silurian	475	Dark gray, fine-grained, silty to sandy dolomitic limestone; bedding is variable, ranging from thick bedded to very thin bedded and platy; several beds of bioclastic limestone and occasional cherty shale interbeds are present in the top one-third of the section in the Carlin trend
Hanson Creek Formation	Ordovician	325	Dark gray to black, fine-grained, thin- to thick-bedded massive dolomite with locally abundant thin beds of black chert; fossil debris beds and intraformational breccias are locally common, especially near the top of the unit
		Disconformity	
Eureka Quartzite	Ordovician	325–500	White, thick-bedded to massive mature sandstone with interbeds of thin- to thick-bedded white, gray, and black sandstone and gray, fine-grained sandy to silty dolomite
		Unconformity	
Pogonip Group	Ordovician	430–600	Blue-gray, thin-bedded, silty limestone at base; grades upward into fine-grained, pale gray cherty limestone; top of unit is thin- to thick-bedded, fine-grained limestone with ribbony shale partings
		Unconformity	
Hamburg Dolomite	Cambrian	>250	Regionally, blue-gray, thin- to thick-bedded dolomite and minor limestone with a few thin quartz siltstone beds; where exposed in the Carlin trend, most of these rocks are metamorphosed to calc-silicate hornfels; base of unit is not exposed

nated silty limestone units of the upper Roberts Mountains Formation and the Popovich Formation, form the major hosts for gold mineralization in the district. Lesser but significant amounts of ore are hosted by the Rodeo Creek formation and igneous rocks. Because drilling at Post-Betze has not penetrated below the Roberts Mountains Formation, the amount of ore present in lower stratigraphic units is unknown.

Radtke (1985) and Madrid and Bagby (1986) described the regional structure of the Carlin trend as a shallowly plunging anticline with an undulatory axis. Several orebodies in the trend are on crests of the undulations along the main axis of the anticline. This large-scale structure predates mineralization and probably acted as a petroleum trap prior to mineralization (Poole et al., 1983; Kuehn, 1989). Elevated temperatures during the Triassic burial resulted in maturation of hydrocarbons in these traps and rendered them essentially immobile prior to mineralization (Kuehn, 1989).

Igneous rocks intruded the Paleozoic sequence in north-central Nevada from Jurassic to late Tertiary time (Stewart, 1980). The intrusions most pertinent to this study are the Goldstrike stock, because of its spatial association with gold ore, and the Welches Canyon stock (Figs. 2 and 3), because of its temporal association with mineralization. Gravity and magnetic data strongly suggest that surface exposures of both stocks only represent a small part of their true size. Tertiary volcanic and plutonic rocks of several ages have been preserved in the Carlin trend area,

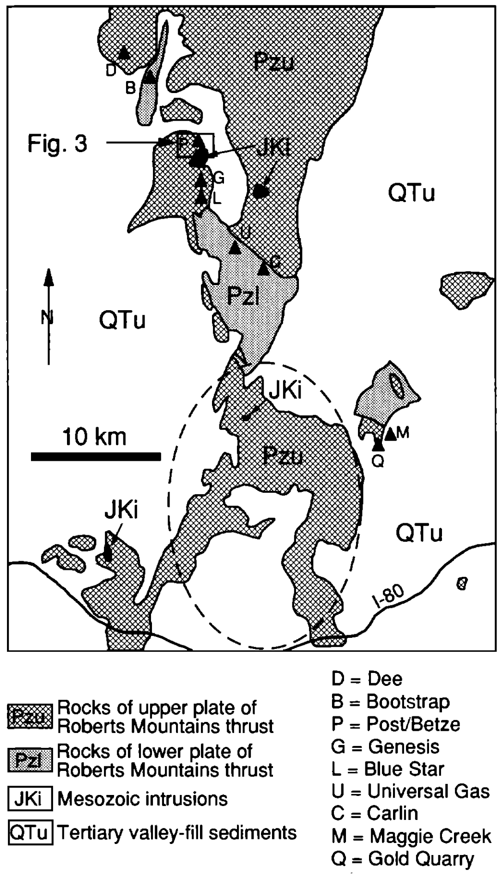

FIG. 2. Generalized geologic map of north-central Nevada, simplified from Stewart and Carlson, (1978). The oval dashed line is the approximate outline of the Welches Canyon pluton, based on magnetic data (Mabey et al., 1978). Dated sample of this pluton is from the JKi outcrop in the north center of the oval. Rain and Alligator Ridge are southeast of this map.

including major igneous episodes at ca. 35 and 17 Ma (Stewart, 1980).

Following and in part coeval with Tertiary igneous activity was the initiation of extensional tectonics of the Basin and Range at about 40 Ma (Atwater, 1970; Stewart, 1980; Zoback et al., 1981; Dallmeyer et al., 1986; Levy and Christie-Blick, 1989). Voluminous sediments shed from the uplifting ranges into intervening valleys during extension between 17 to 6 Ma are collectively known as the Humboldt Formation in the study area. Basin and Range extension continues to the present, with deposition of the Carlin Formation (6-0 Ma) and Holocene sediments overlying the Humboldt Formation.

Geology and Alteration Features of the Post-Betze Deposit

Geology

The Post-Betze deposit consists of several stacked orebodies (Figs. 3 and 4). The deposit (defined as rocks with Au grades in excess of 2.0 g/t) is largely in favorable beds of the Popovich Formation and upper parts of the Roberts Mountains Formation. The sedimentary section is summarized in Table 1 and has been described in detail by Evans (1980).

Lesser amounts of ore occur in igneous rocks of the Goldstrike stock and related dikes. The Goldstrike stock is a composite mesozonal pluton that ranges in composition from granodiorite to granite with local mafic zones. It is generally hypidiomorphic granular in texture and the major minerals are plagioclase, orthoclase, biotite, quartz, and hornblende, with trace amounts of pyroxene. The stock is little altered, except where it has been cut by faults and fractures and where affected by mineralizing fluids along the margins. Surficial weathering is extensive and reaches depths of several hundred meters in and adjacent to fault zones. The age of the Goldstrike stock provides an upper limit on the time of mineralization, but it is poorly known from previous work. Reported K/Ar dates for biotite from the Goldstrike stock range from 78 to 121 Ma (Hausen and Kerr, 1968; Morton et al., 1977). A stock of similar texture and composition across the valley to the east in Little Boulder basin gave a K/Ar date on biotite of 154 Ma (Morton et al., 1977). To define the age of the Goldstrike stock, $^{40}Ar/^{39}Ar$ stepheating analyses were performed on visually fresh (in thin section) mineral separates of unaltered rock away from both hypogene and surficial alteration. These measurements define an apparent age of 158 Ma for the Goldstrike intrusion, as described below.

The Goldstrike stock is cut by numerous preore dikes and sills, up to a few meters thick, that comprise 40 percent of the drill core in places. All of these are

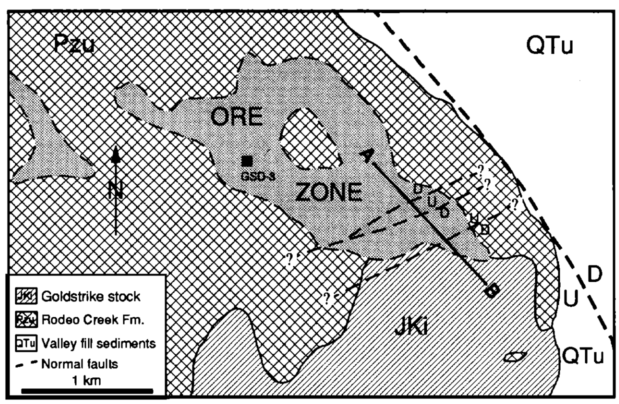

FIG. 3. Generalized geologic map of the Post-Betze area, simplified from unpublished American Barrick and Newmont Mining Company maps and the authors' mapping. The ore zone (gray shaded) has been projected to the surface; the majority of the ore occurs in Pzl rocks at depths between 300 and 500 m. Surface location of sample GSD-3 is shown. Abbreviations as given in Figure 2.

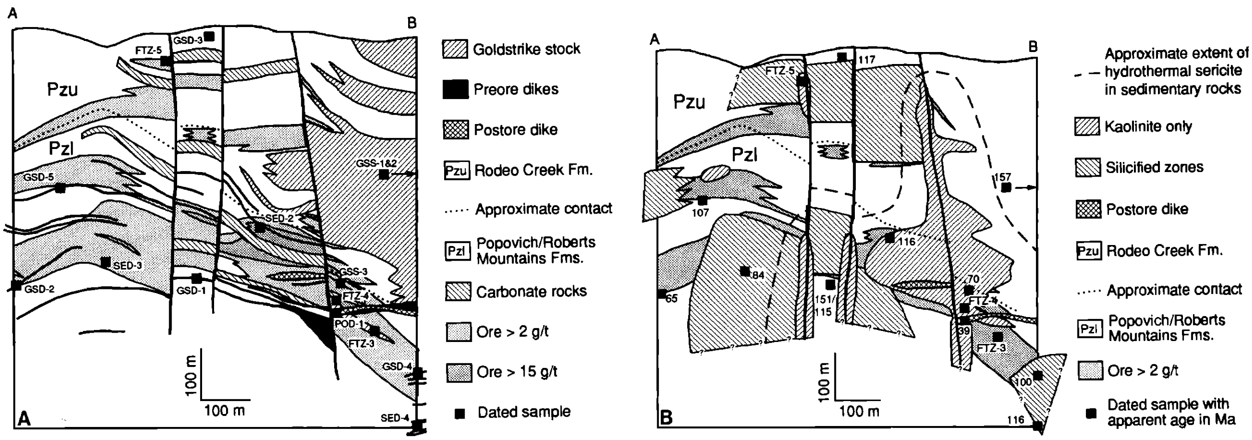

FIG. 4. A. Geologic cross section through the main feeder zone of the Post-Betze system. Nearly all of the rocks shown in this section originally had some carbonate component that was removed by decarbonatization. More massive, less permeable carbonate units were resistant to decarbonatization and can be traced along section as shown. Approximate position of the contact between the Rodeo Creek Formation (Pzu) and the Popovich-Roberts Mountains Formations (Pzl) is shown by heavy dotted line. B. Alteration cross section through the main feeder zone of the Post-Betze system. Both silicification and argillization were controlled by original lithology and the resulting alteration patterns have much more of a "Christmas tree" appearance adjacent to feeder faults, but correlation between holes on the scale of this section is not possible. The most intense argillization, where sericite was altered to kaolinite, was controlled by faults. The boundary between hydrothermal sericite and prehydrothermal sericite is generalized because of a lack of exposure for detailed sampling and the stratigraphic control on alteration.

quartz monzonitic to granitic with textures ranging from aphanitic-porphyritic to fine-grained phaneritic-porphyritic. In several places these dikes are breccias, some of which have fluidized structures. They appear to be sill-like and have been correlated laterally as shown in Figure 4. Most of the dikes have been altered intensely to quartz-sericite mixtures although many retain primary igneous textures. Where present as sills in sedimentary rocks, they acted as barriers to fluid flow and resulted in "ponding" of ore fluids that generated elevated gold grades immediately below them. Nowhere were any dikes found that contain unaltered primary phases that might record meaningful ages. Given the present exposure, the relationships between various textural types of dike are unclear.

The youngest igneous rock in the ore zone is a postmineralization, porphyritic-aphanitic latite sill, first recognized during core logging in 1988 (Figs. 4 and 5). The sill is present in a few drill holes in the center of the orebody, and similar rocks of greater extent (perhaps the parent stock?) are present in drill core from east of the major range front fault. The rock comprises feldspar and biotite phenocrysts set in an aphanitic groundmass. Although feldspar phenocrysts have been altered to fine-grained quartz and sericite, the biotite phenocrysts appear fresh in thin section. The sill bears distinct textural similarities to at least one other dike which is exposed in the district a few kilometers southwest of Post-Betze. The sill cuts ore and locally contains xenoliths of highly mineralized rock. It is barren, however, and a plot of gold grade vs. depth for a core hole shows a dramatic drop in grade across the sill (Fig. 5). Incremental-heating, $^{40}Ar/^{39}Ar$ measurements on primary biotite indicate an age of approximately 39 Ma, as detailed below.

Alteration

Mineralization and alteration were controlled primarily by faults, crests of folds, and permeability of the rocks. The orebodies extend several hundred

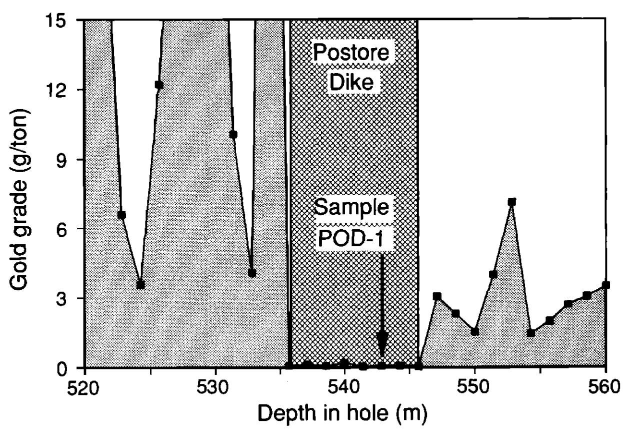

FIG. 5. Plot of gold grade vs. depth for drill hole 213. Gold grades drop to below detection limits within the dike but are of good ore grade on either side. Dated sample (POD-1) is from 543 m.

meters to the northwest of the section shown in Figure 4 and follow stratigraphic horizons, but the zones of most intense mineralization are adjacent to a major fault that served as the predominant conduit for hydrothermal fluids. Ore horizons follow stratigraphy and individual ore horizons can be traced over several thousand meters laterally on the basis of relative grade characteristics. This distribution does not mean that fluid flow necessarily occurred over such lateral distances, because numerous faults probably served as conduits throughout the orebody, and grades are generally higher adjacent to those faults. Igneous rocks and carbonate units having a low percentage of detrital components acted as barriers to fluid flow; higher grade ore intercepts occur in the crests of folds just below impermeable units.

Hydrothermal alteration patterns at Post-Betze include decarbonatization, silicification, and argillization and are similar to those described for other sediment-hosted disseminated gold deposits (e.g., Radtke, 1985; Bakken, 1990; Ilchik, 1990). The earliest alteration was decarbonatization, which removed up to 30 percent of the rock mass in some places, commonly without a concomitant decrease in volume, providing an ideal aquifer for later hydrothermal solutions. In areas of faulting, some compression of the section occurred due to collapse of the decarbonatized rocks. Bakken and Einaudi (1986) describe in detail the relationship between variable decarbonatization and ore at Carlin. Birak (1986) and Ilchik (1990) describe comparable effects at Alligator Ridge and Jerritt Canyon, respectively. Similar relations are seen at Post-Betze, although the detailed geometric relationships cannot be elucidated from present exposures. There is a distinct decrease in the extent of decarbonatized rocks away from faults upsection. Carbonate units having lesser amounts of detrital material had sufficiently low initial permeabilities to resist significant porosity increase by decarbonatization, whereas porosity and permeability were enhanced in silty units that had higher initial permeabilities. This enhanced permeability played a major role in controlling the location of mineralization.

Silicification postdated decarbonatization and also was strongly stratigraphically controlled, particularly on a small scale (Fig. 4B). Products of silicification range from weak veinlet, incipient silicification which is fracture controlled to complete replacement of bedded sedimentary rocks (jasperoid) where sedimentary textures are preserved. Jasperoid breccias, which are common at depth, represent sedimentary slump breccias that originally may have been debris flow breccias (Zimmerman et al., 1987), karst breccias, fault breccias, and explosion breccias that were subsequently silicified. Explosion breccias include silicified diatreme material as well as what appear to be pebble dikes. A better understanding of the geometry and interrelationships between breccias must await better exposures produced during mining.

Phyllosilicates produced during alteration are particularly germane because sericite (used herein to refer to any fine-grained potassium-bearing, iron-poor mica; generally structurally illite or muscovite) can be dated by isotopic methods. Such dates are significant to the age of ore formation only if the sericite is clearly related to mineralization. Phyllosilicate zoning in ore-hosting sedimentary rocks at Post-Betze (Fig. 4B) comprises a core of kaolinite (i.e., sericite destroyed) grading outward into the hydrothermal assemblage kaolinite-sericite (with kaolinite dominant over sericite). The kaolinite-only zone is restricted to the most intensely altered rocks in and adjacent to the major fluid conduits. In the core of the kaolinite zone, dickite is the predominant clay mineral. Stable isotope analyses confirm this kaolinite to be hydrothermal rather than supergene (Arehart et al., 1992).

Outside the core of kaolinite, the sedimentary rocks contain detrital and/or diagenetic kaolinite and sericite, and many rocks contain sericite and kaolinite of both origins. Hydrothermal sericite generally is present only in very small quantities (identifiable petrographically) in most samples outside of the kaolinite core (Fig. 4B). This distribution is similar to the distribution of hydrothermal sericite reported from other sediment-hosted disseminated gold deposits (e.g., Bakken and Einaudi, 1986; Birak, 1986; Ilchik, 1990) and in agreement with the geochemical modeling of Hofstra et al. (1991). Only a few samples of sedimentary rocks having abundant hydrothermal sericite are found at Post-Betze and these are described below.

Regional studies by Harris et al. (1980) and Poole et al. (1983) indicate that the entire area of the Carlin trend experienced prolonged elevated temperatures during the early Mesozoic (Triassic?), probably resulting in recrystallization and upgrading of preore (diagenetic) illites. Data obtained during this study are consistent with this; all X-rayed samples yielded similar, highly crystalline illite 10 Å peaks. Such mixed heritage bulk sericites can be identified and classified into their respective types in thin sections, but they cannot be separated mechanically for analysis. Therefore, it was important to select samples which either are dominated by hydrothermal (new) sericite or are close enough to the core of the system to have been reset completely.

Similar phyllosilicate alteration zoning is present in igneous rocks, although the kaolinite zone is more restricted and hydrothermal sericite is more widespread. This is because potassium was more abundant, and because igneous rocks were less permeable, resulting in lower water/rock ratios, both of which favor stability of sericite. Alteration proceeded from distal chlorite + sericite through sericite + kaolinite to proximal kaolinite only. In terms of mineral separation for dating, the problem of primary igneous sericite is similar to that of primary sedimentary sericite; that is, it is essentially impossible to discriminate between magmatic deuteric and hydrothermal sericite during the mineral separation procedures.

The important relationship in our phyllosilicate alteration studies is the one between zoning and ore. The central kaolinite alteration zone coincides with the main fluid conduit zone for gold mineralization and hydrothermal sericite is most abundant immediately adjacent to this kaolinite zone. Thus sericite samples most likely to yield dates of mineralization were selected from rocks containing the maximum amount of hydrothermal (new) sericite. Samples for dating were carefully selected on the basis of their position in the orebody relative to the alteration zoning, as well as detailed petrographic study, to evaluate their paragenetic position. Several samples contained sericite that was clearly hydrothermal in origin, whereas others contained dominantly (possibly completely) premineralization sericite. Some of the latter samples were selected for analysis to evaluate the possible resetting of sericite.

Analytical Techniques

Potassium/argon and $^{40}Ar/^{39}Ar$

Both K/Ar and $^{40}Ar/^{39}Ar$ techniques were applied following the Ohio State University procedures outlined by Foland et al. (1984), with two notable differences. One is that a Staudacher-type double-vacuum furnace (Staudacher et al., 1978) with precisely controlled temperature and low line blanks was used for $^{40}Ar/^{39}Ar$ incremental heating. The other is that a new $^{40}Ar/^{39}Ar$ technique using encapsulated vials was employed for some very fine-grained samples for which only small amounts of sericite were available. In Table 2, $^{40}Ar/^{39}Ar$ total fusion and incremental-heating analyses are reported for biotite and hornblende from the Goldstrike stock, biotite from a postore sill, and an igneous rock-hosted sericite. K/Ar data for sericites are reported in Table 3. Encapsulated-vial $^{40}Ar/^{39}Ar$ dates are reported for two fine-grained sericites in Table 2.

A major problem with $^{40}Ar/^{39}Ar$ analysis of fine-grained material, such as sericite alteration products in sedimentary rocks (sedimentary sericite), is the recoil loss of ^{39}Ar during irradiation which results in apparent dates that are too old (e.g., Foland et al., 1984). For this reason, conventional K/Ar dating was performed on fine-grained materials that were available in sufficient quantities to yield splits for K and Ar analyses. An encapsulated-vial $^{40}Ar/^{39}Ar$ fusion procedure was developed for fine-grained materials that are available in small amounts, such as hydrothermal sericite from sedimentary rocks associated with sediment-hosted disseminated gold deposits. Although the details of the method are presented elsewhere (Foland et al., 1992), the procedure is described briefly because two dates from this procedure are presented in Table 2.

For the encapsulated-vial analyses, sericites are placed in small high-purity SiO_2 glass vials; these vials are then evacuated and sealed under high vacuum. The small vial retains Ar lost from the sample by recoil during irradiation. These small vials, each containing one unknown sample, are placed inside normal irradiation vials with neutron fluence monitors on each side and irradiated in the normal manner (Foland et al., 1984). After irradiation, the small, sealed vial containing the sericite is dropped into a previously outgassed tantalum crucible of the double-vacuum furnace, which is then slowly heated to 1,300°C. With progressive heating, the sericite decomposes so that the pressure inside the vial increases; eventually with progressive increased pressure (and softening of the glass), the vial ruptures, releasing Ar (both sample Ar and that lost via recoil) into the fusion system. After heating at 1,300°C for 30 mins, the liberated and released Ar is purified and analyzed in the normal manner. The irradiation parameter (J) appropriate to the encapsulated unknown is determined by interpolation of the monitors on each side. The $^{40}Ar/^{39}Ar$ fusion date measured by this procedure should be equated to a K/Ar date. The sericites of Table 2 were analyzed using this procedure.

Samples were irradiated for approximately 100 h in the H5 position of the Ford Nuclear Reactor at the University of Michigan. The monitor used was an intralaboratory biotite standard with a $^{40}Ar/^{39}Ar$ age of 121.7 Ma. An age uncertainty of ±1 percent is assigned to this monitor to provide for the uncertainty of the calibration minerals and is incorporated into the quoted uncertainties. The monitor biotite was calibrated against other standards and relative to it the Mmhb-1 intralaboratory standard gives an age of 513.5 Ma (see Foland et al., 1986, 1989). Factors for the production of interfering Ar isotopes and for K/Ca and K/Cl ratios, as given in Table 2, were determined for the Ford reactor during the interval of analysis.

For K/Ar measurements, all K concentrations were determined in triplicate using lithium metaborate to serve as a flux and to provide an Li internal standard for flame photometry measurements; Ar concentrations were determined in duplicate using a ^{38}Ar tracer delivered by a metering system. Ar extractions for these and $^{40}Ar/^{39}Ar$ total fusion analyses were made on a vacuum system with radio frequency induction heating. Ar extractions for incremental heat-

TABLE 2. Results of $^{40}Ar/^{39}Ar$ Analyses of Post-Betze Samples (samples are described in Appendix)

T[1]	$^{40}Ar/^{39}Ar$[2]	$^{38}Ar/^{39}Ar$[2]	$^{37}Ar/^{39}Ar$[2] (×100)	$^{36}Ar/^{39}Ar$[2] (×100)	F[3]	^{39}Ar[4] (%)	^{40}Ar[5] (%)	K/Ca[6]	K/Cl[7]	Apparent age[8] (Ma) ± 1σ
GSS-1 biotite (150–250 μm, from Goldstrike stock); run 39D9 (J = 0.007950; 0.1148 g)										
>1,200	11.89	0.1195	6.811	0.1671	11.36	100	95.6	7.67	49.2	156.0 ± 1.5
GSS-1 biotite (150–250 μm, from Goldstrike stock); run 39D5 (J = 0.007944; 0.3077 g)										
300	69.06	0.3972	41.48	22.81	1.686	0.02	2.4	1.26	15.3	24.0 ± 9.5
500	6.989	0.0966	41.70	1.075	3.819	1.13	54.6	1.25	63.4	53.9 ± 0.3
575	11.67	0.1083	14.33	0.3520	10.62	2.21	90.9	3.65	54.6	146.1 ± 0.3
650	11.67	0.1113	3.842	0.0820	11.40	7.25	97.7	13.6	52.7	156.4 ± 0.7
725	11.57	0.1103	3.341	0.0326	11.45	11.38	98.9	15.6	53.2	157.0 ± 0.4
775	11.64	0.1103	5.193	0.0246	11.54	6.52	99.2	10.1	53.2	158.2 ± 0.4
815	11.63	0.1113	6.616	0.0424	11.48	4.19	98.7	7.90	52.7	157.5 ± 0.6
855	11.93	0.1143	8.535	0.0425	11.78	4.89	98.8	6.12	51.1	161.4 ± 0.3
900	11.89	0.1154	6.940	0.0311	11.77	6.66	99.0	7.53	50.6	161.3 ± 0.4
960	11.58	0.1164	7.808	0.0255	11.48	17.09	99.2	6.69	50.1	157.5 ± 0.3
1,020	11.45	0.1113	3.645	0.0237	11.35	32.90	99.2	14.3	52.6	155.8 ± 0.5
1.080	11.70	0.1194	23.45	0.0862	11.43	5.44	97.7	2.23	48.8	156.9 ± 0.5
>1,200	41.48	0.1475	155.7	9.830	12.54	0.32	30.2	0.34	44.8	171.4 ± 10.2
Sum	11.65	0.1128	7.261	0.0902	11.36	100	97.5	7.20	51.9	155.9
^{39}Ar age spectrum: Preferred age, 650°–1,080°C (96% of ^{39}Ar)										157.2 ± 1.7
GSS-1 hornblende (150–250 μm, from Goldstrike stock); run 39D6 (J = 0.007960; 0.1163 g)										
>1,200	15.91	0.5092	8.915[9]	1.683[9]	11.69	100	73.1	5.86[9]	10.5	160.6 ± 2.6
GSS-1 hornblende (150–250 μm, from Goldstrike stock); run 39E3 (J = 0.007905; 0.0957 g)										
>1,200	17.30	0.5265	9.006[9]	2.082[9]	11.92	100	68.4	5.80[9]	10.2	162.4 ± 2.2
GSS-1 hornblende (150–250 μm, from Goldstrike stock); run 39D2 (J = 0.007793; 0.4709 g)										
550	31.30	0.2227	6.775[9]	6.112[9]	13.82	2.20	44.0	7.71[9]	26.1	184.5 ± 12.6
650	15.98	0.1043	6.305	1.782	11.24	3.30	70.0	8.29	58.5	151.4 ± 1.5
725	12.04	0.0983	2.964	0.1584	11.81	1.62	97.8	17.6	60.8	158.8 ± 0.3
800	12.93	0.0567	3.215	0.6763	11.18	6.28	86.3	16.3	119.0	150.7 ± 0.4
875	13.63	0.2979	7.371	0.7957	11.91	5.63	86.9	7.09	18.3	160.1 ± 1.7
925	13.13	0.5266	7.971	0.5800	12.11	12.62	91.7	6.56	10.1	162.7 ± 1.2
975	12.11	0.6440	6.694	0.3571	11.63	32.35	95.6	7.81	8.23	156.5 ± 0.8
1,025	12.17	0.5637	5.854	0.3352	11.69	21.02	95.6	8.93	9.43	157.1 ± 0.7
1,075	12.98	0.6239	8.358	0.4906	12.26	9.52	93.9	6.25	8.49	164.6 ± 0.7
1,150	14.48	0.6831	38.21	1.793	12.53	4.65	84.4	1.37	7.64	168.1 ± 3.0
>1,200	180.9	0.7884	139.6	60.20	15.60	0.80	7.8	0.37	7.27	206.9 ± 37.2
Sum	15.09	0.5217	9.113	1.353	11.88	100	78.2	5.74	10.2	159.7
^{39}Ar age spectrum: Preferred age, 875°–1,025°C (72% of ^{39}Ar)									158.1	±2.1
GSS-2 biotite: Run 41M11 (J = 0.007905; 0.3430 g)										
500	119.5	0.3229	55.46	39.27	3.491	0.14	2.92	0.94	21.9	49.1 ± 10.8
600	10.00	0.1022	54.21	0.9028	7.353	3.28	73.50	0.96	58.3	101.9 ± 0.4
640	11.45	0.1173	21.47	0.3534	10.39	2.98	90.80	2.43	49.4	142.5 ± 0.3
675	11.80	0.1233	8.349	0.1648	11.29	7.10	95.71	6.26	46.6	154.2 ± 0.4
720	11.75	0.1240	3.582	0.0790	11.49	7.12	97.82	14.6	46.2	156.9 ± 0.3
750	11.77	0.1344	3.582	0.0587	11.57	6.32	98.34	14.6	42.4	157.9 ± 0.3
780	11.81	0.1253	4.543	0.0229	11.72	5.55	99.24	11.5	45.7	159.9 ± 0.4
825	11.89	0.1263	6.943	0.0442	11.74	7.83	98.74	7.53	45.3	160.1 ± 0.3
900	11.72	0.1264	7.781	0.0331	11.60	27.50	99.00	6.72	45.3	158.4 ± 0.4
975	11.54	0.1244	5.957	0.0270	11.43	29.88	99.13	8.77	46.1	156.2 ± 0.3
1,040	11.73	0.1232	5.034	0.0799	11.46	1.64	97.80	10.4	46.6	156.6 ± 0.4
1,115	13.50	0.1249	7.381	0.5089	11.97	0.47	88.72	7.08	46.2	163.2 ± 0.4
>1,200	19.04	0.1312	6.601	2.191	12.54	0.20	65.89	7.92	45.0	170.6 ± 2.1
Sum	11.80	0.1250	8.412	0.1445	11.35	100	96.22	6.21	45.9	155.1
^{39}Ar age spectrum: Preferred age, 675°–1,115°C (94% of ^{39}Ar)									157.5	1.7

TABLE 2. (*Cont.*)

T[1]	$^{40}Ar/^{39}Ar$[2]	$^{38}Ar/^{39}Ar$[2]	$^{37}Ar/^{39}Ar$[2] (×100)	$^{36}Ar/^{39}Ar$[2] (×100)	F[3]	^{39}Ar[4] (%)	^{40}Ar[5] (%)	K/Ca[6]	K/Cl[7]	Apparent age[8] (Ma) ± 1σ
POD-1 biotite (150–250 μm, from postore dike); run 39D3 (J = 0.007880; 0.1017 g)										
−1,200	3.228	0.0871	4.177	0.1238	2.835	100	87.8	12.5	68.9	39.9 ± 0.4
POD-1 biotite (150–250 μm, from postore dike); run 39E6 (J = 0.007952; 0.0985 g)										
−1,200	2.960	0.0864	4.492	0.0584	2.760	100	93.2	11.6	69.4	39.2 ± 0.4
POD-1 biotite (150–250 μm, from postore dike); run 39D8 (J = 0.007964; 0.4588 g)										
350	22.86	0.0612	7.924	7.056	1.980	0.11	8.7	6.60	148.0	28.2 ± 9.2
525	4.400	0.0592	13.65	0.6292	2.521	2.06	57.3	3.83	111.0	35.9 ± 0.3
600	3.645	0.0913	17.19	0.3505	2.594	2.41	71.2	3.04	65.6	36.9 ± 0.1
675	2.887	0.0823	1.428	0.0550	2.696	7.27	93.4	36.6	73.4	38.3 ± 0.1
730	2.826	0.0792	0.8076	0.0247	2.724	5.84	96.4	64.7	76.6	38.7 ± 0.1
800	2.813	0.0802	0.6002	0.0174	2.732	9.25	97.1	87.1	75.4	38.8 ± 0.1
860	2.839	0.0802	0.9765	0.0192	2.753	11.79	97.0	53.5	75.4	39.1 ± 0.1
920	2.819	0.0823	1.472	0.0148	2.746	9.14	97.4	35.5	73.3	39.0 ± 0.1
970	2.782	0.0802	1.938	0.0111	2.721	18.05	97.8	27.0	75.4	38.7 ± 0.1
1,020	2.773	0.0823	3.017	0.0122	2.710	18.61	97.7	17.3	73.3	38.5 ± 0.1
>1,200	3.133	0.0993	10.63	0.1328	2.720	15.47	86.8	4.92	59.3	38.7 ± 0.1
Sum	2.933	0.0836	3.716	0.0644	2.716	100	92.6	14.1	72.0	38.6
^{39}Ar age spectrum: Preferred age, 675°–>1,200°C (95% of ^{39}Ar)									38.8	±0.4
GSD-1 sericite (20–40 μm, from preore dike); run 39E8 (J = 0.007962; 0.0988 g)										
>1,200	10.76	0.0171	0.0796	0.0910	10.47	100	97.27	6.57	883.0	144.5 ± 1.5
GSD-1 sericite (20–40 μm, from preore dike); run 40I5 (J = 0.007901; 0.1270 g)										
475	35.47	0.0447	0.0136	10.14	5.475	1.22	15.44	38.3	355.0	76.4 ± 1.3
525	10.88	0.0171	0.0043	1.005	7.881	2.16	72.46	120.0	1,250.0	109.0 ± 1.5
575	8.912	0.0129	0.0066	0.1524	8.430	3.47	94.63	78.7	3,260.0	116.3 ± 0.7
600	9.460	0.0110	0.0151	0.1002	9.132	3.85	96.57	34.7	>5,000.0	125.7 ± 0.5
640	10.10	0.0115	0.0062	0.0232	10.01	9.38	99.04	84.2	>5,000.0	137.3 ± 0.3
680	10.59	0.0116	0.0087	0.0065	10.55	14.35	99.55	60.4	>5,000.0	144.4 ± 0.3
720	10.91	0.0114	0.0110	0.0019	10.88	17.54	99.69	47.7	>5,000.0	148.7 ± 0.3
760	11.08	0.0142	0.0137	0.0095	11.03	18.01	99.50	38.3	1,660.0	150.7 ± 0.3
800	11.14	0.0121	0.0022	0.0028	11.11	12.10	99.68	240.0	4,640.0	151.7 ± 0.3
850	11.11	0.0122	0.0076	0.0028	11.08	7.69	99.67	68.7	4,360.0	151.4 ± 0.3
>1,200	11.24	0.0430	0.0044	0.1202	10.87	10.23	96.67	120.0	164.0	148.6 ± 0.6
Sum	11.07	0.0159	0.0086	0.1725	10.53	100	95.15	61.0	1,150.0	144.2
GSD-1 sericite (40–100 μm, from preore dike); run 41M8 (J = 0.007895; 0.3292 g)										
500	20.95	0.0427	0.7879	5.637	4.259	0.31	20.34	66.3	247.0	59.7 ± 11.8
575	10.83	0.0205	0.4854	0.9320	8.041	2.99	74.28	108.0	673.0	111.0 ± 0.7
600	8.988	0.0130	0.2126	0.1354	8.556	11.08	95.20	246.0	2,990.0	117.9 ± 0.3
640	9.378	0.0121	0.3269	0.0563	9.180	11.23	97.89	160.0	>5,000.0	126.2 ± 0.3
675	9.942	0.0112	0.1618	0.0276	9.829	20.40	98.86	323.0	>5,000.0	134.8 ± 0.3
720	10.44	0.0112	0.1304	0.0187	10.35	21.70	99.17	401.0	1,000.0	141.7 ± 0.3
750	10.68	0.0116	0.2070	0.0199	10.59	11.74	99.16	253.0	>5,000.0	144.9 ± 0.3
780	10.78	0.0116	0.3752	0.0218	10.68	8.05	99.11	139.0	>5,000.0	146.1 ± 0.3
825	10.77	0.0118	0.0323	0.0297	10.65	5.34	98.89	1,620.0	>5,000.0	145.6 ± 0.3
880	10.67	0.0119	0.5854	0.0622	10.44	3.97	97.88	89.3	>5,000.0	142.9 ± 0.3
>1,200	8.099	0.0157	2.949	0.2669	7.281	3.19	89.91	17.7	1,240.0	100.8 ± 0.4
Sum	10.11	0.0122	0.3121	0.0934	9.802	100	96.96	167.0	>5,000.0	134.5

TABLE 2. (*Cont.*)

T[1]	$^{40}Ar/^{39}Ar$[2]	$^{38}Ar/^{39}Ar$[2]	$^{37}Ar/^{39}Ar$[2] (×100)	$^{36}Ar/^{39}Ar$[2] (×100)	F[3]	^{39}Ar[4] (%)	^{40}Ar[5] (%)	K/Ca[6]	K/Cl[7]	Apparent age[8] (Ma) ± 1σ
GSD-1 sericite (40–100 μm, from preore dike); run 41L9 (J = 0.007832; 0.2991 g)										
475	19.86	0.0229	1.125	4.413	6.790	2.56	34.20	46.47	493	93.5 ± 1.9
550	8.989	0.0126	0.0391	0.1775	8.433	10.82	93.84	1,336.0	4,197	115.4 ± 0.3
600	9.310	0.0115	0.2840	0.0463	9.141	9.93	98.21	184.0	>5,000	124.7 ± 0.3
640	9.747	0.0116	0.0678	0.0235	9.645	12.93	98.98	770.7	>5,000	131.4 ± 0.3
680	10.23	0.0116	0.0717	0.0103	10.17	15.73	99.41	728.5	>5,000	138.2 ± 0.3
710	10.64	0.0113	0.0333	0.0073	10.59	14.70	99.52	1,569.0	>5,000	143.7 ± 0.3
740	10.90	0.0117	0.3078	0.0025	10.87	11.90	99.66	169.8	>5,000	147.3 ± 0.3
770	11.03	0.0119	0.0064	0.0045	10.99	7.41	99.61	8,149.0	>5,000	148.9 ± 0.3
800	11.01	0.0174	0.0128	0.0316	10.89	4.15	98.89	4,069.0	827	147.6 ± 0.3
850	10.66	0.0131	0.0180	0.0312	10.54	3.31	98.86	2,903.0	2,602	143.0 ± 0.3
>1,200	8.913	0.0179	0.0450	0.3276	7.914	6.56	88.82	1,161.0	832	108.5 ± 0.3
Sum	10.35	0.0128	0.1273	0.1669	9.823	100.00	94.95	410.0	3,431	133.7
SED-3 sericite[10] (<2 μm, from subore sedimentary rocks); run 41E10 (J = 0.007843; 0.0298 g)										
>1,200	20.40	1.312	12.27	4.854	6.140		30.10	4.26	4.04	84.9 ± 1.7
SED-4 sericite[10] (<2 μm, from low-grade sedimentary rocks); run 41E9 (J = 0.007645; 0.0253 g)										
>1,200	11.63	1.859	46.67	1.046	8.700		74.77	1.12	2.83	116.2 ± 1.3

[1] Temperature in °C; sum = summation of all fractions
[2] The isotope ratios given are not corrected for Ca-, K-, and Cl-derived Ar isotope interferences; ^{37}Ar has been corrected for decay using a half-life of 35.1 d
[3] F is the ratio of radiogenic ^{40}Ar to K-derived ^{39}Ar; it is corrected for atmospheric argon and interference using the following factors: $(^{40}Ar/^{36}Ar)_{AIR} = 295.5$, $(^{39}Ar/^{37}Ar)_{Ca} = 6.510 \times 10^{-4}$, $(^{36}Ar/^{37}Ar)_{Ca} = 2.70 \times 10^{-4}$, $(^{40}Ar/^{39}Ar)_K = 0.0329$, $(^{38}Ar/^{39}Ar)_K = 0.0121$, $(^{36}Ar/^{38}Ar)_{Cl} = 2.01754 \times 10^{-6}$/d
[4] Relative percent of the total ^{39}Ar released by fraction
[5] Percent of the total ^{40}Ar in the fraction that is radiogenic
[6] Wt ratio calculated using the relationship: $K/Ca = 0.523 \times (^{39}Ar_K/^{37}Ar_{Ca})$
[7] Wt ratio calculated using the relationship: $K/Cl = 5.220 \times (^{39}Ar_K/^{38}Ar_{Cl})$
[8] Ages calculated using a ^{40}K total decay constant of 5.543×10^{-10} yr^{-1}; for steps of incremental heating analyses, provision for systematic J uncertainty is omitted; a relative ±1% J uncertainty is included in the uncertainties of all total fusion and indicated preferred ages
[9] For hornblende, the given $^{37}Ar/^{39}Ar$ and $^{38}Ar/^{39}Ar$ ratios are not ×100; the K/Ca ratio is ×100
[10] Sample analyzed by the encapsulated-vial technique described by Foland et al., 1992

ing analyses and the encapsulated-vial procedure were performed on another system in a double-vacuum furnace. All Ar measurements were performed using a Nuclide SGA-6-60 mass spectrometer operated in the static mode by an on-line minicomputer.

The sizes of the analyzed mineral separates are given in Tables 2 and 3. Most sericite concentrates are from the <2-μm-diam-size fraction. Separation of fine-grained sericites was accomplished by grain settling in water followed by centrifugation. Although this method incorporates minor impurities of quartz and kaolinite, other potassium-bearing minerals (primarily potassium feldspar) were effectively eliminated.

Fission track

Following mineral separation by standard heavy-liquid techniques, fission track ages of apatite and zircon were determined using the external detector method (Naeser, 1976, 1979). The single apatite mineral separate was mounted in epoxy, polished, and then etched in 7 percent HNO_3 at 23°C for 40 s. Zircon grains were mounted in teflon, polished, and etched in a eutectic melt of KOH-NaOH (Gleadow et al., 1976) at 215°C for 30 to 50 h. The teflon mounts containing the zircons were covered with a muscovite detector and irradiated along with U-doped glass SRM-962 as a neutron dose monitor. The apatite mount was also covered with muscovite and irradiated with U-doped glass SRM-963. These glass dose monitors are described by Carpenter and Reimer (1974). Samples were irradiated in the U. S. Geological Survey reactor at Denver, Colorado. The dose was determined from the track density in the muscovite detectors that covered the glass standard during the irradiations. Ages were calculated using the Zeta method of calibration and calculation as recommended by Hurford and Green (1983). The fission track data and ages are reported in Table 4.

TABLE 3. K and Ar Analytical Data and Calculated Ages for Sericite Samples from Sediment-Hosted Disseminated Gold Deposits, Nevada

Sample[1]	K (wt %)	$^{40}Ar_{rad}$ (10^{-10} mole/g)	$^{40}Ar_{rad}/^{40}Ar_{total}$	Calculated age[2] (Ma)
MCC-3	1.57	5.79	0.64	
	1.59	5.62	0.58	
	1.58	5.39	0.67	
Avg	1.58	5.60		194 ± 5
SED-2 (5.8)	4.96	10.35	0.93	
	5.00	10.32	0.90	
	4.94			
Avg	4.97	10.33		116 ± 2
GSS-3 (47.7)	2.87	3.50	0.82	
	2.85	3.60	0.86	
	2.86			
Avg	2.86	3.55		70 ± 1
GSD-1 (0.6)	6.49	16.85	0.97	
	6.49	16.91	0.97	
Avg	6.49	16.88		144 ± 2
GSD-2 (0.4)	5.24	5.96	0.81	
	5.21	5.97	0.88	
	5.19			
Avg	5.21	5.97		65 ± 1
GSD-3 (7.9)	6.09	12.80	0.64	
	6.07	12.67	0.67	
	6.07			
Avg	6.08	12.74		117 ± 2
GSD-4 (2.1)	3.81	6.67	0.92	
	3.80	6.93	0.89	
	3.80			
Avg	3.80	6.80		100 ± 2
GSD-5 (3.4)	3.92	7.43	0.74	
	3.90	7.50	0.86	
	3.89			
Avg	3.90	7.47		107 ± 2

[1] Samples: MCC-3 = unaltered Roberts Mountains Formation; SED-2 = high-grade sedimentary rock-hosted ore, sericite dominated by hydrothermal material; GSS-3 = high-grade ore within the Goldstrike stock; GSD-1 = poststock, preore dike; GSD-2 = fluidized breccia postore dike containing clasts of ore; GSD-3 = preore dike from Long Lac pit; GSD-4 = highly altered preore dike; GSD-5 = thin preore dike in sedimentary section; numbers in parentheses are gold grades in grams/ton; more detailed descriptions are given in Appendix

[2] Constants used: $^{40}K = 1.167 \times 10^{-2}$ atom percent of total K; $(^{40}Ar/^{36}Ar)_{AIR} = 295.5$; $\lambda_e = 0.581 \times 10^{-10}$ yr^{-1}; $\lambda_{\beta^-} = 4.962 \times 10^{-10}$ yr^{-1}; analytic uncertainties quoted are $\pm 1\sigma$

K/Ar and $^{40}Ar/^{39}Ar$ Results

The objectives of this study were to bracket the time of mineralization by dating biotite and hornblende from both pre- and postmineralization igneous rocks, and to date the sericite that is interpreted to be related to mineralization from both igneous and sedimentary host rocks.

For the $^{40}Ar/^{39}Ar$ stepheating analyses, none of the samples yielded concordant age spectra or plateau for which apparent age differences (for a large portion of ^{39}Ar released) may be attributed solely to analytical errors. Nevertheless, several samples give spectra with broad plateaulike portions that have only minor discordance. Although the exact cause of the discordance is not clear, it is probably caused by mineralogical heterogeneities such as minor alteration of biotite. For these samples, the discordance may be the product of, for example, ^{39}Ar recoil redistribution during irradiation. Therefore, a preferred age is herein defined as the age determined from continuous gas fractions weighted by the relative amounts of ^{39}Ar using the criteria: (1) 90 percent or more of the ^{40}Ar of a fraction is radiogenic, (2) all fractions are within $\pm 3\ \sigma$ of the apparent stepheating age, (3) steps collectively constitute more than 50 percent of the total ^{39}Ar, and (4) the K/Ca and K/Cl ratios of the gas fractions are relatively uniform. Viewed in perspective, the degree of age discordance of the fractions used to define the preferred age is small and minor compared to the apparent age differences among samples.

Preore stock

Two samples of the unaltered Goldstrike stock were dated by $^{40}Ar/^{39}Ar$ total fusion and stepheating techniques (Table 2; Fig. 6). Sample GSS-1 is from monzonite of the Goldstrike stock at a depth of 300 m and several hundred meters from any known or inferred mineralization; sample GSS-2 is from a slightly more felsic phase from a depth of 727 m in the same hole. For the hornblende separate from sample GSS-1, a stepheating age of 158.1 ± 2.1 was produced for the fractions released between 875° and 1,025°C (Table 2). The high-temperature fractions from this sample yield slightly older ages, probably as a function of small amounts of included impurities, particularly pyroxene, as indicated by the low K/Ca ratio of these fractions (Fig. 6A). A biotite separate from the same sample yielded a preferred age of 157.2 ± 1.7 Ma (Fig. 6B). For sample GSS-1, the hornblende and biotite ages are indistinguishable at the 95 percent confidence level. Biotite from sample GSS-2 gave a preferred age of 157.5 ± 1.7 Ma (Fig. 6C), which is also indistinguishable.

These analyses establish an age of about 158 Ma for the Goldstrike stock and, at the same time, set important constraints on mineralization. First, because the differences between hornblende and biotite dates are negligible, the Goldstrike stock apparently cooled quickly through the interval of hornblende and biotite closure to Ar loss (approx 500° and 300°C, respectively; McDougall and Harrison, 1988). Second, heating during mineralization apparently did not exceed the temperatures necessary to reset biotite for any significant period of time. Finally, these ages constrain mineralization to be post-158 Ma because portions of the Goldstrike stock are intensely mineralized.

TABLE 4. Zircon and Apatite Fission Track Data for Samples from the Post-Betze Area

Sample[1]	No. of grains	ρ_s[2]	Fossil tracks	ρ_i[2]	Induced tracks	χ^2[3]	Tracks counted	Age (Ma)	Uncertainty $\pm 1\sigma$
GSS-1(z)	7	10.3	1,676	4.74	384	F	2,701	132	8
GSS-1(z)	*1*	*8.94*	*414*	*5.53*	*128*			*98*	*12*
GSS-1(z)	*6*	*10.9*	*1,262*	*4.42*	*256*	*P*		*149*	*11*
FTZ-2(z)	3	8.44	430	3.02	77	P	2,701	169	21
FTZ-3(z)	7	22.9	2,124	10.4	483	F	2,701	133	7
FTZ-3(z)	*2*	*24.9*	*808*	*14.9*	*242*	*P*		*101*	*8*
FTZ-3(z)	*5*	*21.9*	*1,316*	*8.01*	*241*	*P*		*165*	*12*
FTZ-4(z)	8	6.09	1,437	3.07	362	F	2,701	120	8
FTZ-4(z)	*6*	*5.00*	*880*	*2.85*	*251*	*P*		*106*	*8*
FTZ-4(z)	*2*	*9.25*	*557*	*3.69*	*111*	*P*		*152*	*16*
POD-1(z)	6	3.35	590	480	455	P	2,701	43	3
POD-1(a)	7	0.218	108	2.45	607	P	5,075	41	4
MCC-3(z)	8	7.99	888	9.97	544	F	2,701	49	3
MCC-3(z)	*4*	*6.70*	*527*	*11.9*	*468*	*P*		*34*	*2*
MCC-3(z)	*1*	*8.86*	*41*	*7.78*	*18*			*69*	*20*
MCC-3(z)	*3*	*11.5*	*320*	*4.90*	*68*	*P*		*142*	*19*

[1] Samples: GSS-1 = fresh Goldstrike stock; FTZ-2 = altered Goldstrike stock, average grade 1.9 g/t Au; FTZ-3 = altered Goldstrike stock, average grade 24 g/t Au; FTZ-4 = sandy sedimentary rocks from 5420 bench, 12000 E, 12075 N, average grade 2.2 g/t Au; POD-1 = postore dike; MCC-3 = fresh Roberts Mountains Formation from Maggie Creek Canyon; more detailed descriptions are given in Appendix; (z) = zircon separates; (a) = apatite separates; data shown in italics are subpopulations of the larger data set for that sample

[2] $\rho \times 10^6$ tracks/cm^2; ρ_s = spontaneous track density, ρ_i = induced track density

[3] Pass (P) or fail (F) χ^2 test at 5 percent (external detector runs); dosimeter density for all samples = 1.925×10^5 t/cm^2 except POD-1(a) where density = 0.430×10^5 t/cm^2

Postore sill

A sample of the postore sill (POD-1; see Fig. 4) was dated by $^{40}Ar/^{39}Ar$ total fusion and by stepheating of biotite phenocrysts (Table 2, Fig. 6D). Two fused samples have ages of 39.9 ± 0.4 and 39.2 ± 0.4 Ma. The preferred age of this sample is 38.8 ± 0.4 Ma and is not significantly different from the total fusion age. The 39 Ma date clearly establishes a lower limit on the time of mineralization.

Altered igneous rocks

Six samples of sericite from altered igneous rocks were dated by K/Ar methods (Table 3, Fig. 4); one of these (GSD-1) was considered coarse grained enough to yield $^{40}Ar/^{39}Ar$ stepheating results not rendered meaningless by ^{39}Ar recoil loss. Five samples were taken from various preore dikes or Goldstrike stock in or near the main ore zone, and the sixth was taken from a dike in a near-surface ore zone.

Sample GSD-3 (7.9 g/t Au), a near-surface sample from the Long Lac pit (Figs. 3 and 4A), gave a K/Ar age of 117 ± 2 Ma. Sample GSD-5 (3.4 g/t Au), from a dike in the northwesternmost portion of the cross section (Fig. 4), yielded a K/Ar age of 107 ± 2 Ma. Sample GSD-4 (2.1 g/t Au), from one of a group of dikes in the southeastern portion of the orebody (Fig. 4), gave a K/Ar age of 100 ± 3 Ma.

Sample GSD-2 is from the northwestern portion of the section of Figure 4; sericite from this rock has a K/Ar age of 65 ± 1 Ma. This rock appears to be a distal fluidized breccia equivalent of the postore sill, and it thus should be much younger than mineralization. The 1.6-m interval from which this sample was taken carries a grade of 0.4 g/t Au but contains only 80 percent igneous rock. Although it is immediately adjacent to some of the highest grade mineralization in the hole (in the 1.6-m interval below the sample, sedimentary rock contains 4.3 g/t Au), both the age and gold grades are inferred to reflect a mixture of predike sedimentary rocks and postore sill igneous material. Because of the fluidized breccia character of the rock, the determined age is considered to be a composite or mixed age which is not geologically meaningful.

Sample GSS-3 (47.7 g/t Au) is the only available sample of the main portion of the Goldstrike stock that contained sufficient sericite for analysis. A K/Ar age of 70 ± 2 Ma was determined for sericite from this rock. The sample was taken 20 m above the postore sill, which is 12 m thick in this hole. Given normal rock porosities and permeabilities this separation may be sufficient to obviate thermal resetting. However, the rocks in this portion of the orebody have been completely decarbonatized and intensely sheared and clearly have been the locus of hydrothermal circulation. Therefore, we suggest that the sericite in this sample has been partially reset by the thermal effect of the postore sill, and as such, the date does not reflect a geologic event at 70 Ma.

Sample GSD-1 (0.6 g/t Au) comprises sericite from a preore igneous dike slightly below the main ore

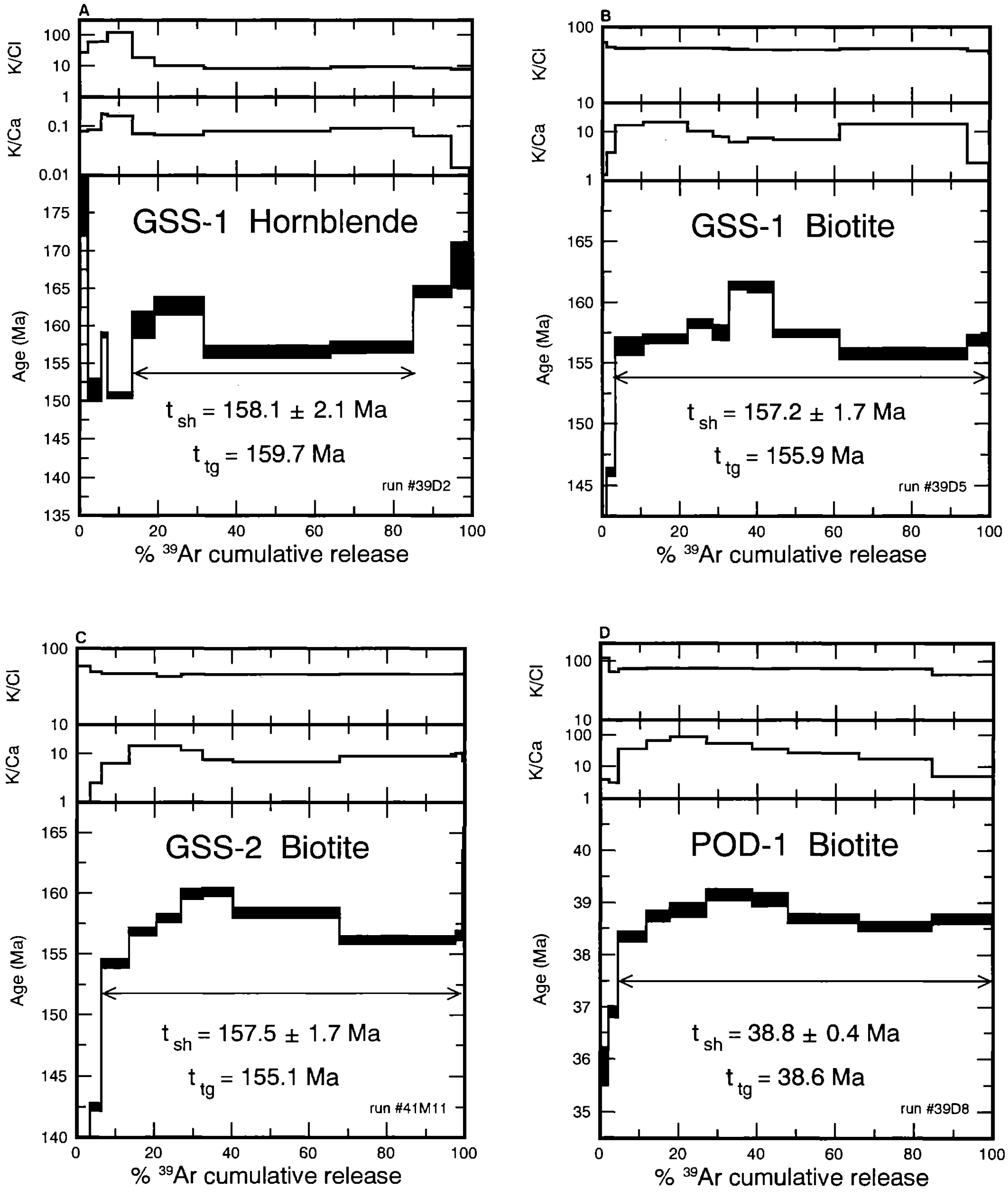

FIG. 6. Stepheating analyses of mineral separates. t_{sh} = preferred age for the fractions shown by the arrow, t_{tg} = total gas age; large variations in K/Ca and K/Cl reflect the presence of mineral impurities in the sample. Width of bars represents 1σ uncertainties. A. Hornblende mineral separate from fresh Goldstrike stock. Sample GSS-1, from drill hole ST7 at 297-m depth. B. Biotite mineral separate from fresh Goldstrike stock. Sample GSS-1, from drill hole ST7 at 297-m depth. C. Biotite mineral separate from fresh Goldstrike stock. Sample GSS-2, from drill hole ST7 at 727-m depth. D. Biotite mineral separate from postore dike. Sample POD-1, from drill hole 213 at 543-m depth.

zone. This is the only sample that contained sericite of sufficient size to attempt stepheating analysis. Two different size fractions were analyzed: a 20- to 40- and a 40- to 100-μm diam. For the sample containing sericites from 20 to 40 μm in diam, statistically identical ages were determined by K/Ar (144 ± 2 Ma; Table 3) and $^{40}Ar/^{39}Ar$ total fusion techniques (144.5 ± 1.5 Ma; Table 2). The general concordance of these ages is strong evidence that ^{39}Ar recoil loss is not a problem for this sample. The coarser (40- to 100-μm) fraction yielded a total gas age (integrated from stepheating analyses) of 134 ± 1.5 Ma. Not only are total gas ages for the two size fractions different but also the age spectra are distinctly discordant. The incremental heating results are similar for the two sizes; apparent ages increase progressively with the heat-

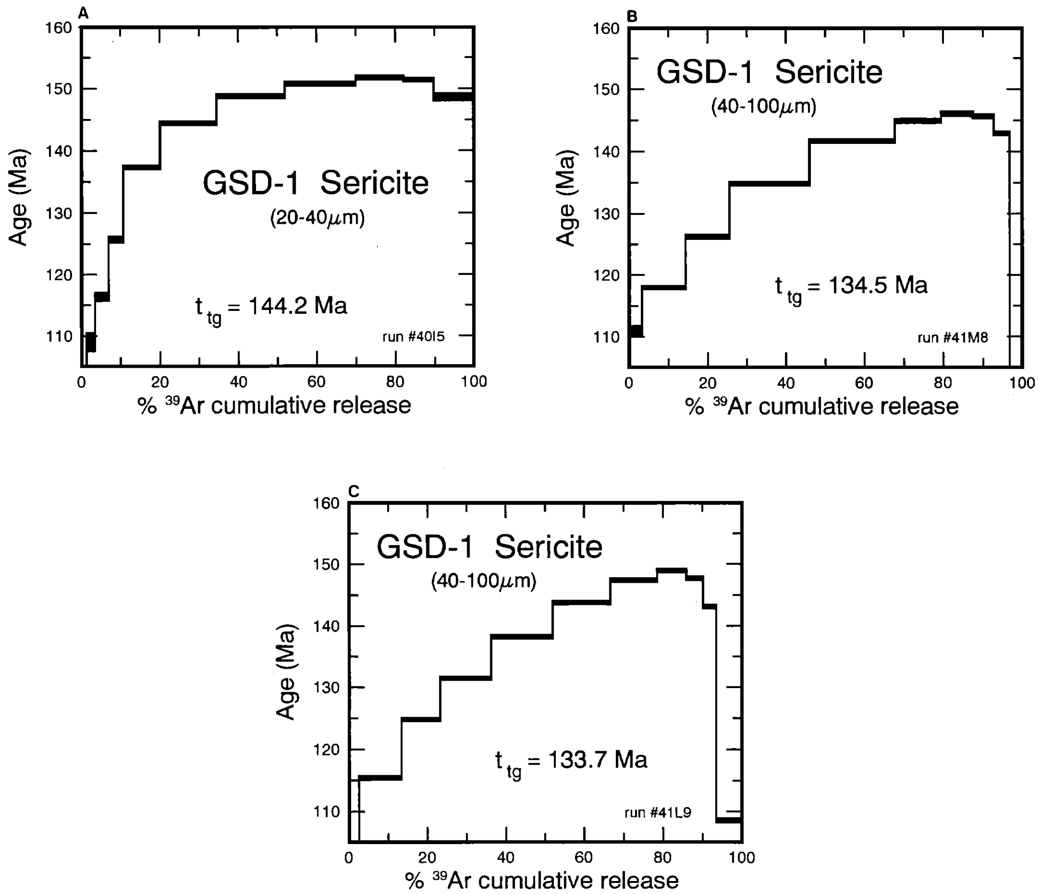

FIG. 7. Stepheating analysis of sericite from a preore dike below the main mineralized zone. Sample GSD-1, from drill hole 118 at 491-m depth. A. 20- to 40-μm-size fraction; B. and C. 40- to 100-μm-size fraction. Width of bars represents 1σ uncertainties.

ing temperature starting at about 110 Ma and reaching approximately 150 Ma (Fig. 7). The spectrum for the 20- to 40-μm fraction has an apparent maximum at 151.2 ± 1.5 Ma at high temperatures. The 40- to 100-μm fraction spectra that reach ca. 146 to 149 Ma at high temperature are followed by a decrease in age for small fractions at the highest extraction temperature. The decrease in apparent age at high temperatures for these three separates probably reflects degassing of minor impurities, such as feldspar, as indicated by accompanying decreases in K/Ca and K/Cl ratios.

The simplest explanation of these spectra is that they reflect gas release of two sericite populations or components, one of which has an age of ca. 113 Ma and the other having an age of ca. 150 Ma. The differences in Ar results for the 20- to 40- vs. 40- to 100-μm fractions, therefore, reflect merely a difference in the relative proportions of the two components in these size fractions. Whether the younger component represents new sericite generated during hydrothermal events or simple resetting of some preexisting grains (or their margins) as a result of thermal disturbance is unclear. In thin sections large sericite grains generally comprise a single domain core surrounded by finer grained multiple domain rims. We suggest that the large cores are the remnants of deuteric alteration at approximately the time of dike emplacement, whereas the rims are hydrothermal sericite formed during the mineralizing event. Although we favor the hypothesis that the youngest ages represent the time of mineralization, it is possible that these ages are the result of a thermal disturbance that is much younger than 113 Ma, a thermal event that only partially reset the K/Ar clock and fortuitously produced an age of approximately 113 Ma. This, however, seems highly unlikely because the apparent older and younger ages are the same for both size fractions which, on the basis of total gas ages, clearly have different relative proportions of the various components. It seems that sample GSD-1 provides evidence for sericite formation and/or resetting at 150 and 113 Ma.

Unaltered sedimentary rocks

Sample MCC-3 of unaltered silty limestone of the Roberts Mountains Formation was collected from Maggie Creek Canyon, approximately 25 km southeast of the Post-Betze deposit, to provide some constraints on the age of altered sedimentary sericites from within the deposit. Sericite from this sample gave a conventional K/Ar date of 194 ± 5 Ma (Table 3). We interpret this date to reflect essentially complete resetting of the sericite by regional metamorphism during the Triassic accretion of Sonomia (Speed, 1979). It serves to rule out the possible contribution of much older sericite (either Paleozoic or Precambrian) to the ages determined on Post-Betze sedimentary samples.

Altered sedimentary rocks

In addition to the unaltered sedimentary rock sample described above, three sericite samples from altered sedimentary rocks were analyzed by conventional K/Ar or the encapsulated-vial technique. These samples were selected to provide analyses ranging from high relative proportions of hydrothermal sericite to those with very little hydrothermal sericite.

Sample SED-2 is a dark gray, partially silicified sedimentary rock from the high-grade ore zone (5.8 g/t Au) obtained as close to the center of the hydrothermal system as possible (Fig. 4). This sample was chosen carefully to maximize the probability that all sericite present was hydrothermal in origin. In thin section, sericite from this sample clearly is intergrown with, and locally occurs in fractures cutting, auriferous pyrite. The K/Ar age of this sample is 116 ± 2 Ma (Table 3).

Mineral separates from two other samples were of insufficient mass to date by conventional K/Ar methods but were dated by the encapsulated-vial $^{40}Ar/^{39}Ar$ fusion procedure. Sample SED-4 (0.1 g/t Au) is from an intensely sheared and comminuted sedimentary rock from below the main ore zone. Although it does not host ore-grade material, this sample was selected because of its locally abundant hydrothermal sericite in thin section and because of its proximity to the center of the hydrothermal system. A single sericite + quartz separate from this sample was dated at 116.2 ± 1.3 Ma. Sample SED-3 (0.2 g/t Au) is a medium gray, decarbonatized rock from the Roberts Mountains Formation below the main ore zone. In thin section, nearly all of the sericite from this sample appears to be detrital. The apparent age of the sericite concentrate from this sample is 84.9 ± 1.7 Ma, an age that is not concordant with any other dates from the deposit. Although not observed during analysis of the sample, possible Ar-loss errors associated with the encapsulated-vial technique (see Foland et al., 1992, for more discussion) could potentially produce the anomalously young age. As an alternative explanation, 5 m above the sample is a 2-m-thick sill of unknown age that had been interpreted as preore because of its intense alteration; it is possible that the sill is postore and caused disturbance of the K/Ar system. Because of these unresolved questions, we do not consider this age a reliable indicator of a particular geologic event.

Alunite

It has been suggested that the alunite present in sediment-hosted disseminated gold deposits is associated genetically with gold (Radtke, 1985; Ilchik, 1990; Rota and Hausen, 1991). K/Ar dates reported from two samples of Post-Betze alunite are 8.6 ± 0.2 and 9.5 ± 0.2 Ma (Arehart et al., 1992). These ages indicate that alunite formed significantly later than the postore sill and they confirm the lack of any genetic relation between alunite and gold at this locality. Textural relationships and stable isotope data from these alunites, and from alunite from numerous other sediment-hosted disseminated gold deposits, are in agreement with the conclusion that alunite in these deposits is supergene in origin (Arehart et al., 1992).

Zircon and Apatite Fission Track Results

Although the fission track annealing properties of zircon are not well known, several estimates have been made for the closure (annealing) temperature; Harrison et al. (1979) estimate 175°C and Hurford (1986) estimates 240° ± 50°C. Additionally, experience has shown (C. W. Naeser, unpub. data) that there is a correlation between uranium contents and fission track ages of individual zircon grains from rocks that have been moderately heated. The closure temperature for apatite is thought to be near 100°C (Naeser, 1976, 1979). Because these temperatures are at or below those generally accepted for sediment-hosted disseminated gold hydrothermal systems (e.g., Radtke, 1985; Kuehn, 1989), the hydrothermal system should have reset the fission track ages in both detrital and igneous minerals. Presuming that no later thermal event again reset the ages, fission track ages of preore apatite should reflect an age of cooling following mineralization, and zircon may do so also.

Six samples were selected for fission track analyses of apatite and zircon (Fig. 4, Table 4). All of these samples contained zircon, but only one (POD-1) contained recoverable apatite. Zircon ages have unimodal distributions in only two of the samples. Both of these samples passed the χ^2 test at the 95 percent confidence level, indicating single populations (Naeser and Crowley, 1989). The four other samples all failed the χ^2 test, indicating that there may be more than a single age group present in the sample population. The presence of two or more populations can be explained by partial annealing of the crystals. If a zircon suite is heated to partial annealing temperatures, grains with higher uranium content will be affected more than those with low uranium content and consequently yield younger ages. Such a correlation between age and uranium content is present (see Table 4) in three of the four nonunimodal samples. Age is negatively correlated with induced track density, except for sample FTZ-4 where all populations have relatively low track densities.

Sample POD-1 is from the postore sill; both apatite and zircon ages passed the χ^2 test, indicating unimodal populations. Zircon gives an age of 43 ± 3 Ma, and apatite gives an age of 41 ± 5 Ma. Both of these dates are within uncertainty of the postore sill $^{40}Ar/^{39}Ar$ age of 39 Ma. These data also demonstrate that there has been no significant thermal activity since ca. 39 Ma. Because sediment-hosted disseminated gold deposits are believed to form at temperatures of at least 180°C (e.g., Radtke, 1985; Kuehn, 1989), the lack of any resetting in either mineral confirms the lower age limit of 39 Ma for mineralization.

Three zircon separates from the Goldstrike stock were analyzed. A zircon sample from the fresh monzonite (GSS-1) failed the χ^2 test based upon the entire sample population. However, if a single outlier is dropped from the sample set, an age of 149 ± 11 Ma is obtained. This age, within uncertainties, is consistent with that obtained by $^{40}Ar/^{39}Ar$ stepheating. The only unimodal sample (FTZ-2) is from weakly mineralized stock and has an age of 169 ± 21 Ma. The error on this age is large because only three grains were suitable for analysis. This age also is in general agreement and within analytical error of the $^{40}Ar/^{39}Ar$ date for the stock. The third Goldstrike sample (FTZ-3) is from a heavily mineralized portion of the orebody. This sample failed the χ^2 test; separation of this zircon sample into two subpopulations indicates ages of 165 ± 12 and 101 ± 8 Ma.

Two samples from the sedimentary section were analyzed: one from mineralized rock in the pit (FTZ-4: 2.3 g/t Au), and a sample from Maggie Creek Canyon, approximately 30 km southeast of the mine (MCC-3). Although it failed the χ^2 test, sample MCC-3 has a large subpopulation, having an age of 34 ± 3 Ma. Several individual grains having ages ranging between 69 and 167 Ma were present in the sample; all of these grains had low uranium contents. Although the K/Ar systems of detrital micas apparently have not been affected, annealing of most of the detrital zircons has occurred, probably due to documented igneous activity in the vicinity. Zircons having high uranium contents have been completely annealed, whereas those containing lesser amounts of uranium have been only partially annealed.

The single sedimentary sample from Post-Betze failed the χ^2 test; separation of this sample into subpopulations, based upon uranium content, results in a bimodal distribution of ages at 106 ± 8 and 152 ± 16 Ma.

Discussion of $^{40}Ar/^{39}Ar$ and K/Ar Dates

$^{40}Ar/^{39}Ar$ stepheating dates

On the basis of stepheating analyses of biotite and hornblende from the Goldstrike stock and postore sill, the ages of these igneous events seem well established, in spite of minor discordance in the age spectra. The $^{40}Ar/^{39}Ar$ ages are further supported by fission track results. The Goldstrike preferred ages for hornblende (158.1 ± 1.5 Ma) and biotite (157.2 ± 1.7 and 157.5 ± 1.7 Ma) are not analytically distinct. For the postore sill, the ages for biotite (38.8 ± 0.41 Ma) and zircon and apatite (43 ± 3 and 41 ± 5 Ma, respectively) are identical within analytical uncertainties. The concordance of the dates for these minerals with different closure temperatures is strong support that they measure the times of cooling of the magmas. Therefore, these data conclusively bracket the time of mineralization to be between 158 and 39 Ma.

The interpretation of the sericite dates with respect to the timing of mineralization is more problematic because of the possibilities that samples may contain some inherited material of an older age and/or that they may have been reset by some thermal or hydrothermal event younger than mineralization. The stepheating results for sericite separates from altered Goldstrike dike sample GSD-1 are consistent with the presence of two populations of sericite. Indeed, petrographically this sample contains two distinct populations of sericite and is the only one to do so. The age of 151 Ma observed for higher temperature increments sets a minimum age for the closure of the older sericite component; the 158 Ma age of the stock sets a maximum age for this component. It seems likely that this sericite was generated as a result of magmatic deuteric alteration or hydrothermal alteration associated with skarn mineralization but not during main-stage gold mineralization. The stepheating analyses do not define clearly an age for the younger sericite component, but the results are consistent with a maximum age near 110 to 115 Ma. This sericite may have formed at a temperature below that of Ar blocking, during gold mineralization. Alternatively, the event is potentially significantly younger and produced partial thermal resetting of 151 to 158 Ma deuteric sericite.

The two size fractions of sample GSD-1 give different total gas ages, indicating that the smaller (20-40 μm) size fraction contains more of the older sericite component than the larger (40-100 μm) size fraction. The smaller fraction also has a higher K content, indicating that it is purer or that the sheet silicates in it contain more K. This could reflect the cores of large, older sericite grains which were resistant to comminution during mechanical separation processes. Alternatively, it is possible that during hydrothermal events, some process such as Ostwald ripening (Ostwald, 1900; Eberl and Sródon, 1988) took place, whereby larger, composite grains grew at the expense of smaller ones. Such a process also could result in the observed age differences.

K/Ar and $^{40}Ar/^{39}Ar$ fusion dates

It seems likely, in general, that the <2-μm-size fraction is largely new sericite generated as a result of gold-related hydrothermal alteration. However, the possibility that these dates represent a mixture of sericites of varying ages, and do not represent a geologic event at the time as measured, must be considered. For sedimentary rock-hosted sericite, three potential reservoirs of older sericite exist: (1) detrital Precambrian sericite of at least 1.7 Ga age (e.g., lead provinces of Zartman, 1974), (2) diagenetic sericite of roughly Ordovician age, or (3) reset sedimentary (detrital + diagenetic) sericites of post-Ordovician age. Because sericite from unaltered Roberts Mountains Formation (sample MCC-3, Tables 1 and 2) gives a 194 Ma K/Ar date, neither of the two older reservoirs are expected to contribute to the ages determined for sedimentary samples. Therefore, calculations were done incorporating four ages of sericite: sedimentary sericite of 194 Ma; magmatic deuteric sericite of 158 Ma, associated with Goldstrike magmatism; a hypothetical gold-related hydrothermal sericite of 117 Ma; and hydrothermal sericite of 39 Ma (postore sill) age. The calculations were done assuming the same K concentration for both components of sericite.

Three possibilities must be considered: either the dates as measured are too young or too old with respect to actual geologic events, or the dates do not correspond to any geologic event. Dates which are too young may be the result of either partial resetting of an older component or growth of new sericite and mixing of the two types. Dates which are too old must represent inclusion of prehydrothermal sericite in the sample that was analyzed.

First, consider inclusion of an older component in a sample of 117 Ma hydrothermal sericite. Addition of sericite of either 158 or 194 Ma could result in a minor shift in the analytic age relative to the hydrothermal age. Given the observed scarcity of preore sericite in sedimentary rock ($\ll$1%) and the amount of sericite in most analyzed samples (10–15%), the contribution from old sericite is unlikely to have an effect on the age beyond a few million years. An analytical age of 117 Ma is shifted by only 9 m.y. by the inclusion of 10 percent of old sedimentary sericite. Addition of 10 percent of 158 Ma sericite only shifts the analytical age by 4 m.y. and 20 percent shifts it by only 10 m.y. In none of the samples (except GSD-1, discussed above) was there petrographic evidence for a second population of sericite. In sum, the ages of sericite samples, except GSD-1, are not affected substantially (by more than about 10 m.y.) by the possible inclusion of sedimentary or Goldstrike-age sericite.

Addition of sericite of postore sill age (by either resetting or new growth) to a 117 Ma hydrothermal sericite would act to lower the apparent age of mineralization. As noted above, there is no petrographic evidence for a second generation of hydrothermal sericite in the samples analyzed, therefore we reject new growth as a possibility. Because closure temperature, and thus degree of resetting, may be a function of grain diameter, it is possible that partial resetting of fine-grained hydrothermal sericites took place at distances farther from the dike than those deduced for coarse-grained muscovite (McDougall and Harrison, 1988). Several samples are known or inferred to be partially reset. The most obvious example of such postore sill-related thermal disturbance is GSS-3, which has been partially reset and has an age of 70 Ma which we interpret to be geologically meaningless. Samples GSD-4 and GSD-5 also appear to have been subjected to partial resetting. Sample SED-3 may have been subjected to resetting as discussed previously. There is no clear evidence that other samples have been reset; however, the variability in the ages (Tables 2 and 3) may be the result of thermal disturbance.

A final possibility is that the dates we obtained represent only a mixture of old and young sericite and that no hydrothermal event took place at ca. 117 Ma. If this is the case, the two most likely possibilities for the age of mineralization are 158 Ma (associated with intrusion of the Goldstrike stock) or about 40 Ma (just prior to intrusion of the postore sill). We do not think either of these possibilities has strong supporting evidence. An analytical age of 117 Ma requires subequal proportions of old sericite (158-194 Ma) and young sericite (40 Ma). As noted above, most samples do not show petrographic evidence of two generations of sericite. Moreover, the clustering of several ages near 117 Ma from diverse samples also argues against a random mixture of sericite of two ages.

The sericite ages we consider to be most reliable are those from strongly mineralized areas of the orebody and for which petrographic evidence favors a hydrothermal origin for the sericite. Indeed, the two most strongly mineralized sedimentary rock samples

(SED-2 and SED-4; Tables 2 and 3) both have ages of 116 Ma. The highest grade dike sample (GSD-3) has an age of 117 Ma, and the first release fraction from sample GSD-1 has an apparent age of about 113 Ma. The concordance of dates from these samples, obtained from samples widely separated in space, suggests that they record a distinct geologic event, that is, the hydrothermal system responsible for gold mineralization. In addition, two other dike samples which contain ore-grade gold have ages of 107 and 100 Ma, explicable by modest resetting probably associated with the intrusive event that generated the postore sill. Several other samples are known or inferred to have younger apparent ages because of either resetting or growth of new sericite at approximately 40 Ma. In summary, based on the K/Ar and $^{40}Ar/^{39}Ar$ data presented here, we favor an age of approximately 117 Ma for gold mineralization at Post-Betze.

Discussion of Fission Track Data

As discussed above, for thermally disturbed zircon samples, fission track ages and uranium content tend to be inversely correlated. Such patterns are also apparent in the Post-Betze samples. Although the errors on individual grain analyses are large, the patterns of fission track data record the occurrence of two thermal events at Post-Betze after intrusion of the Goldstrike stock. Many of the individual grain analyses cluster between 100 and 115 Ma, similar to K/Ar and $^{40}Ar/^{39}Ar$ ages from alteration minerals. All of these younger grains have high uranium contents, relative to other grains from the same sample. Perhaps most important, these samples yield no evidence of a thermal event on the scale of the entire Post-Betze orebody, occurring after about 100 Ma. In addition, the great spread in individual grain dates suggests that these zircons resided for some time within the partial track annealing zone (150°–250°C), an interpretation that is consistent with other temperature estimates for sediment-hosted disseminated gold deposit formation.

Another way to look at the zircon ages is through the use of a probability density distribution plot (Zeitler et al., 1982, 1988; Hurford et al., 1984; Kowallis et al., 1986; Cerveny et al., 1988). A normal curve is calculated from the age and standard error of the age for each grain that is dated in a sample. The curves for all of the grains in a single sample are then added together to obtain the probability density curve for the sample as a whole. The probability curve for a sample is calculated according to: $A = \sum_{i=1}^{n} \frac{[(A - \bar{A}_i)^2/2s_i^2]}{\sqrt{2\Pi s_i}}$, where A = age, A_i = mean age for zircon i, and s_i = standard error of the mean age for the ith zircon. The cumulative probability curve gives a visual indication of whether more than one population of ages is present in a data set.

The cumulative probability curves for the five samples from the Post-Betze deposit are presented in Figure 8. The three dashed lines represent the approximate ages for three known or suspected events (39, 117, and 158 Ma) that occurred at Post-Betze; peaks in the probability density distribution curves tend to be associated with these three times.

Timing of Mineralization at Post-Betze

Given the constraints discussed above, we consider the best estimate of the timing of mineralization at the Post-Betze deposit to be 117 Ma with an estimated uncertainty of no more than a few million years. This uncertainty is the result of currently unresolved questions about inherited sericite and potential resetting on K/Ar and $^{40}Ar/^{39}Ar$ samples and statistical uncertainties associated with fission track data, probably as a result of variable annealing properties. It also is notable that, with the exception of sample GSS-3, which has probably been reset by the postore sill, all samples having dates near 117 Ma contain significant gold concentrations (i.e., were strongly affected by the hydrothermal system). Only

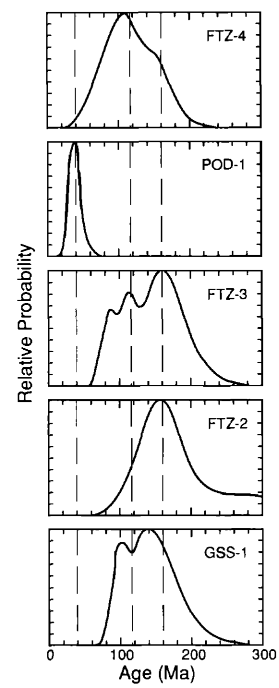

FIG. 8. Cumulative probability density distribution for the zircon ages from the five samples from the Post-Betze deposit. The three dashed lines represent the approximate ages for three known or suspected events that occurred at Post-Betze: intrusion of the postore dike at 39 Ma, inferred age for mineralization at 117 Ma, and intrusion of the Goldstrike stock at 158 Ma.

samples having lower gold contents yield anomalous dates.

There is no igneous body in the immediate vicinity of the deposit that is the obvious thermal driving force for generation of the Post-Betze deposit. Because it formed about 40 m.y. earlier, the Goldstrike stock can be eliminated as a possible thermal source. However, the large Welches Canyon stock is only a few kilometers to the south (Fig. 2). Biotite from this intrusion has been dated by K/Ar methods at 109 Ma (Evans, 1980; recalculated using the tables of Dalrymple, 1979). The date reported was from an undescribed but weathered, surface sample, and therefore its accuracy is difficult to evaluate. Within present attendant uncertainties on the times of emplacement of the Welches Canyon stock and Post-Betze gold mineralization, it is possible that they are the same age. In any event, it is significant that documented igneous activity was occurring in close spatial and temporal proximity to the Post-Betze hydrothermal activity described herein. It seems reasonable to postulate that a pluton similar to, but smaller than, the Welches Canyon stock was emplaced below the Goldstrike stock during the same time period, creating a thermal anomaly that resulted in generation of the Post-Betze hydrothermal system.

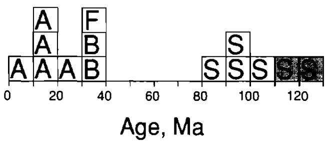

FIG. 9. Histogram of published ages of minerals associated with sediment-hosted disseminated gold deposits. Only a single age has been selected for each deposit; where multiple ages have been reported (Table 5), an average date, or the date thought to be most closely associated with mineralization, has been used. Letters represent the phase dated: A = alunite, B = biotite, F = K feldspar, S = sericite. With the exception of Post and possibly Carlin (shaded boxes), the temporal relationship of the samples dated to mineralization is regarded as highly speculative.

Relationship of Sediment-Hosted Disseminated Gold Deposits to Igneous Activity and Tectonic Environment in the Western United States

Timing of mineralization

Judging from the complexities demonstrated here for Ar dates, considerable uncertainties exist about ages of mineralization of other sediment-hosted disseminated gold deposits. Available radiometric dates from other sediment-hosted disseminated gold deposits in Nevada (Table 5, Fig. 9) encompass a large time range. However, two groups of dates in Table 5, those for alunite, and for biotite and feldspar, are almost certainly not representative of the time of mineralization. Alunite associated with sediment-hosted disseminated gold deposits has been demonstrated to be supergene in origin, on the basis of paragenesis and stable isotope measurements (Arehart et al., 1992). The alunite ages, which range from 8.6 to 30 Ma, serve only to provide minimum ages for mineralization. The second group of dates, which clusters near 35 Ma, is from fresh minerals from rocks that are spatially associated with mineralization. Because these dates are from fresh minerals (biotite and sanidine) that are normally altered to sericite or kaolinite in sediment-hosted disseminated gold hydrothermal systems, the dates probably do not record the age of mineralization, a point noted by most authors in presenting the original data.

The remaining data are from sericites. Although the relationship between these sericites and gold mineralization in other deposits is, in some cases, still equivocal, all dates fall between 85 and 125 Ma. This suggests that there may have been a time period (perhaps even more restricted than is implied by this range of dates) and possibly a tectonic environment that was more favorable for the development of sediment-hosted disseminated gold deposits.

During the middle Cretaceous, northeastern Nevada was in a compressional tectonic regime and formed a part of the hinterland of the Sevier overthrust belt (Stewart, 1980). Igneous activity associated with the development of the Sierra Nevadan arc was taking place farther west in Nevada and California. Plutonism of this age also is common in northern Nevada (e.g., Coats and McKee, 1972; Sharpless and Albers, 1987). These dates are significantly older than the earliest dates hypothesized for extensional tectonism in the western United States. Although Davis (1980) suggested that evidence exists for extensional tectonism in western North America north of the Great Basin at ca. 80 Ma, post-Paleozoic extension in the Great Basin is generally thought to have begun in the early Eocene (ca. 37-45 Ma: Dallmeyer et al., 1986; Levy and Christie-Blick, 1989). We suggest, then, that extensional environments are not requisite for (but are not necessarily prohibitive of) the generation of sediment-hosted disseminated gold deposits. Similar deposits from other areas of the world (e.g., Bau: Sillitoe and Bonham, 1990; Yauricocha: Alvarez and Noble, 1988; Guizhou: Ashley et al., 1991) are not associated with extensional regimes.

Mineral deposit alignments

Age constraints provided by our data permit more specific speculation about the origin of the alignment of sediment-hosted disseminated gold deposits in Nevada, a subject that has been widely debated (e.g., Roberts, 1960; Gilluly, 1976; Bagby and Berger, 1985; Percival et al., 1988; Seedorff, 1991). Two crustal structural trends approximately parallel the position of the two major mineral belts (Carlin and Cortez trends; Fig. 1) and have been hypothesized to exert some control on deposit location. Late-stage

TABLE 5. Compilation of Isotopic Ages for Sediment-Hosted Disseminated Gold Deposits

Deposit	Age[1] (Ma)	Description and comments
Alligator Ridge	10–12	K/Ar on alunite considered by some to be hypogene (Ilchik, 1990)
Carlin	58	K/Ar on sericite in dike adjacent to main pit (Morton et al., 1977)
Carlin	123	$^{40}Ar/^{39}Ar$ stepheating on sericite from altered dike (Kuehn, 1989)
Carlin	134	K/Ar on altered dike, Carlin pit; probably preore, thus date is maximum for mineralization (Morton et al., 1977)
Chimney Creek	90–130	K/Ar on sericite and alunite considered to be primary alteration minerals (Osterberg, 1990)
Cortez	36	K/Ar on biotite and sanidine from altered, mineralized felsic porphyry (Wells et al., 1969; Morton et al., 1977)
Getchell	92	K/Ar on sericite from altered, mineralized grandiorite from south pit (Berger and Taylor, 1980)
Gold Acres	95–101	K/Ar on sericite in altered quartz monzonite from core 500 ft below pit; relationship to gold ore uncertain; upper age is from biotite in main stock (Silberman and McKee, 1971)
Gold Quarry	25–30	K/Ar on alunite considered by some to be hypogene (Rota and Hausen, 1991; Arehart et al., 1992)
Mercur	32	K/Ar on biotite from altered rhyolite porphyry; temporal relation to ore is equivocal (Tooker, 1985)
Northumberland	84	K/Ar on sericite; relationship to mineralization not described (Bonham, 1985)
Northumberland	158	K/Ar on biotite from Northumberland stock; relation to mineralization not described (Silberman and McKee, 1971)
Post-Betze	117	This study
Rabbit Creek	15	Alunite from fault zone (Bloomstein et al., 1991)
Rain	20	K/Ar on alunite considered by some to be hypogene (Arehart et al., 1992)
Tenabo	36	K/Ar on sanidine from rhyolite porphyry dike "spatially associated with mineralization" (Silberman and McKee, 1971)

[1] Pre-1977 ages have been recalculated using more recent decay constants (Dalrymple, 1979)

back-arc (or early transform) extensional features include the northern Nevada rift and other aeromagnetic anomalies and the long-wave gravity feature in east-central Nevada (Mabey et al., 1978; Eaton, 1984). They are probably younger than 80 Ma (Davis, 1980), although the age of gravity and aeromagnetic features is difficult to determine. Major right-lateral strike-slip zones are present from the San Andreas and Walker Lane on the south to the Basin and Range boundary faults on the north (Lawrence, 1976; Stewart, 1980; McKee and Noble, 1986). They are probably younger than 45 Ma, the onset of strike-slip interaction between the Pacific and North American plates.

It is clear that the 85 to 125 Ma age of mineralization precludes any direct causal relationship between these tectonic features and gold deposits. However, it has been suggested that precursors to documented strike-slip features existed throughout the Basin and Range, including the area of sediment-hosted disseminated gold deposits (Shawe, 1965; Madrid and Bagby, 1986). We suggest that alignments of mineral deposits, if real, must represent fairly long-lived and deep features in the crust which have controlled thermal properties and intrusive activity on a regional scale through geologic time. At least in Nevada, these features appear to be related to the Precambrian craton margin, because the deposits are distributed symmetrically with respect to this feature (Fig. 1).

Conclusions

Although there is a significant spread in the age data, we suggest that mineralization at Post-Betze took place near 117 Ma. This conclusion is based upon what we consider to be the most reliable K/Ar, $^{40}Ar/^{39}Ar$, and fission track ages of a variety of igneous and sedimentary rocks. Intrusions of this general age are present in northeastern Nevada, including a major pluton nearby at Welches Canyon (109 Ma). We suggest that an intrusion of similar age provided the thermal driving force for generation of the hydrothermal system responsible for mineralization at Post-Betze and other associated deposits.

Based on the available age constraints, we suggest that sediment-hosted disseminated gold deposits are not necessarily products of extensional environments and, in fact, most appear to be associated with compressional environments in Nevada during Cretaceous time. The alignment of sediment-hosted disseminated gold deposits (and other features) in the Basin and Range province of the western United States suggests that zones of long-term crustal weakness may have controlled igneous intrusion and consequent thermal anomalies leading to hydrothermal gold mineralization, although not all igneous episodes necessarily generated sediment-hosted disseminated gold ore deposits. The strong association between sediment-hosted disseminated gold deposits, the Precambrian craton, and these deep-seated structures also suggest the possibility of a deep source for gold and other components of these systems.

Acknowledgments

This study has benefited from discussions with numerous geologists including Larry Kornze, Keith Bettles, and Eric Lauha at American Barrick Resources, Chuck Zimmerman and Jeff Huspeni at Newmont Mining Company, and Skip Cunningham, Hal Bonham, and Al Berry. John Chesley provided much constructive criticism regarding the problems of dating fine-grained sericites. Fritz Hubacher was instrumental in assisting the senior author in mastering the intricacies of Ar analyses, as well as the development of the encapsulated-vial technique. This research was supported financially by grants from American Barrick Resources, the National Science Foundation (EAR-89-05107), Sigma Xi, the Geological Society of America, and the University of Michigan Turner Fund. The Newmont Mining Company provided partial summer salary for the senior author during 1988. J. R. O'Neil, D. R. Peacor, and John Chesley provided constructive criticism on early drafts of the manuscript. We gratefully acknowledge three detailed and insightful comments by *Economic Geology* reviewers, which resulted in significant improvements in the manuscript.

October 21, 1991; November 9, 1992

REFERENCES

Alvarez A., A., and Noble, D. C., 1988, Sedimentary rock-hosted disseminated precious metal mineralization at Purisima Concepcion, Yauricocha district, central Peru: ECON. GEOL., v. 83, p. 1368–1378.

Arehart, G. B., Kesler, S. E., O'Neil, J. R., and Foland, K. A., 1992, Evidence for the supergene origin of alunite in sediment-hosted micron gold deposits: ECON. GEOL., v. 87, p. 263–270.

Ashley, R. P., Cunningham, C. G., Bostick, N. H., Dean, W. E., and Chou, I.-M., 1991, Geology and geochemistry of three sedimentary-rock-hosted disseminated gold deposits in Guizhou province, People's Republic of China: Ore Geology Rev., v. 6, p. 133–151.

Atwater, T., 1970, Implications of plate tectonics for the Cenozoic tectonic evolution of western North America: Geol. Soc. American Bull., v. 81, p. 3513–3535.

Bagby, W. C., and Berger, B. R., 1985, Geologic characteristics of sediment-hosted, disseminated, precious-metal deposits in the western United States: Rev. Econ. Geology, v. 2, p. 169–202.

Bakken, B. M., 1990, Gold mineralization, wall-rock alteration, and the geochemical evolution of the hydrothermal system in the main orebody, Carlin mine, Nevada: Unpub. Ph.D. thesis, Stanford Univ., 236 p.

Bakken, B. M., and Einaudi, M. T., 1986, Spatial and temporal relation between wall rock alteration and gold mineralization, main pit, Carlin gold mine, Nevada, U.S.A., *in* Macdonald, A. J., ed., Gold '86: Willowdale, Ontario, Konsult Internat. Inc., p. 388–403.

Berger, B. R., and Taylor, B. E., 1980, Pre-Cenozoic normal faulting in the Osgood Mountains, Humboldt County, Nevada: Geology, v. 8, p. 594–598.

Bettles, K. H., 1989, Gold deposits of the Goldstrike mine, Carlin trend, Nevada: Soc. Mining Engineers Preprint 89–158, 14 p.

Birak, D. J., 1986, Exploration and geologic development of the Jerritt Canyon gold deposits, Elko County, Nevada, U.S.A., *in* Macdonald, A. J., ed., Gold '86: Willowdale, Ontario, Konsult Internat. Inc., p. 488–496.

Bloomstein, E. I., Massingill, G. L., Parratt, R. L., and Peltonen, D. R., 1991, Discovery, geology and mineralization of the Rabbit Creek gold deposit, Humboldt County, Nevada, *in* Raines, G. L., Lisle, R. E., Schafer, R. W., and Wilkinson, W. H., eds., Geology and ore deposits of the Great Basin: Reno, NV, Geol. Soc. Nevada, p. 821–843.

Bonham, H. F., 1985, Characteristics of bulk-mineable gold-silver deposits in cordilleran and island-arc settings: U. S. Geol. Survey Bull. 1646, p. 71–77.

—— 1986, Bulk-mineable precious-metal deposits and prospects in Nevada: Nevada Bur. Mines Geology Map 91, scale 1:1,000,000.

Carpenter, B. S., and Reimer, G. M., 1974, Calibrated glass standards for fission-track use: Natl. Bur. Standards Spec. Pub. 260–49, p. 1–16.

Cerveney, P. F., Naeser, N. D., Zeitler, P. K., Naeser, C. W., and Johnson, N. M., 1988, History of uplift and relief of the Himalaya during the past 18 million years: Evidence from fission-track ages of detrital zircons from sandstones of the Siwalik Group, *in* Kleinspehn, K. L., and Paola, C., eds., New perspectives in basin analysis: New York, Springer-Verlag, p. 43–61.

Coats, R. R., and McKee, E. H., 1972, Ages of plutons and types of mineralization, northwestern Elko County, Nevada: U. S. Geol. Survey Prof. Paper 800-C, p. C165–C168.

Dallmeyer, R. D., Snoke, A. W., and McKee, E. H., 1986, The Mesozoic-Cenozoic tectonothermal evolution of the Ruby Mountains, East Humboldt Range, Nevada: A cordilleran metamorphic core complex: Tectonics, v. 5, p. 931–954.

Dalrymple, G. B., 1979, Critical tables for conversion of K-Ar ages from old to new constants: Geology, v. 7, p. 558–560.

Davis, G. A., 1980, Problems of intraplate extensional tectonics, western United States, *in* Continental tectonics: Washington, Natl. Academy Sci., p. 84–95.

Eaton, G. P., 1984, The Miocene Great Basin of western North America as an extending back-arc region: Tectonophysics, v. 102, p. 275–295.

Eberl, D. D., and Sródon, J., 1988, Ostwald ripening and interparticle-diffraction effects for illite crystals: Am. Mineralogist, v. 73, p. 1335–1345.

Elison, M. L., Speed, R. C., and Kistler, R. W., 1990, Geologic and isotopic constraints on the crustal structure of the northern Great Basin: Geol. Soc. America Bull., v. 102, p. 1077–1092.

Evans, J. G., 1980, Geology of the Rodeo Creek NE and Welches Canyon quadrangles, Eureka County, Nevada: U. S. Geol. Survey Bull. 1473, 81 p.

Farmer, G. L., and DePaolo, D. J., 1983, Origin of Mesozoic and Tertiary granite in the western United States and implications for pre-Mesozoic crustal structure: I. Nd and Sr isotopic studies in the geocline of the northern Great Basin: Jour. Geophys. Research, v. 88, p. 3379–3401.

Foland, K. A., Linder, J. S., Laskowski, T. E., and Grant, N. K., 1984, $^{40}Ar/^{39}Ar$ dating of glauconites: Measured ^{39}Ar recoil loss from well crystallized specimens: Isotope Geosci., v. 2, p. 241–264.

Foland, K. A., Gilbert, L. A., Sebring, C. A., and Chen, J.-F., 1986, $^{40}Ar/^{39}Ar$ ages for plutons of the Monteregian Hills, Quebec: Evidence for a single episode of Cretaceous magmatism: Geol. Soc. America Bull., v. 97, p. 966–974.

Foland, K. A., Chen, J.-F., Linder, J. S., and Henderson, C. M. B., 1989, High-resolution $^{40}Ar/^{39}Ar$ chronology of multiple intrusion igneous complexes. Application to the Cretaceous Mount Brome complex, Quebec, Canada: Contr. Mineralogy Petrology, v. 102, p. 127–137.

Foland, K. A., Hubacher, F. A., and Arehart, G. B., 1992, $^{40}Ar/^{39}Ar$ dating of very fine-grained samples: An encapsulated-vial proce-

dure to overcome the problem of ^{39}Ar recoil loss: Isotope Geosci., v. 102, p. 269–276.
Gilluly, J., 1976, Lineaments—ineffective guides to ore deposits: ECON. GEOL., v. 71, p. 1507–1514.
Gleadow, A. J. W., Hurford, A. J., and Quaife, R. D., 1976, Fission track dating of zircon: Improved etching techniques: Earth Planet. Sci. Letters, v. 33, p. 273–276.
Harris, A. G., Wardlaw, B. R., Rust, C. C., and Merrill, G. K., 1980, Maps for assessing thermal maturity (conodont color alteration index maps) in Ordovician through Triassic rocks in Nevada and Utah and adjacent parts of Idaho and California: U. S. Geol. Survey Misc. Geol. Inv. Map I-1249, scale 1:2,500,000.
Harrison, T. M., Armstrong, R. L., Naeser, C. W., and Harakal, J. E., 1979, Geochronology and thermal history of the Coast Plutonic Complex, near Prince Rupert, British Columbia: Canadian Jour. Earth Sci., v. 16, p. 400–410.
Hausen, D. M., and Kerr, P. F., 1968, Fine gold occurrence at Carlin, Nevada, *in* Ridge, J. D., ed., Ore deposits of the United States 1933–1967 (Graton-Sales vol.): New York, Am. Inst. Mining, Metall. Petroleum Engineers, p. 908–940.
Hofstra, A. H., Leventhal, J. S., Northrop, H. R., Landis, G. P., Rye, R. O., Birak, D. J., and Dahl, A. R., 1991, Genesis of sediment-hosted disseminated-gold deposits by fluid mixing and sulfidization: Chemical-reaction-path modeling of ore-depositional processes documented in the Jerritt Canyon district, Nevada: Geology, v. 19, p. 36–40.
Hurford, A. J., 1986, Cooling and uplift patterns in the Lepontine Alps, south central Switzerland and an age of vertical movement on the Insubric fault line: Contr. Mineralogy Petrology, v. 92, p. 413–427.
Hurford, A. J. and Green, P. F., 1983, The zeta age calibration of fission-track dating: Isotope Geosci., v. 1, p. 285–317.
Hurford, A. J., Fitch, F. J. and Clarke, A., 1984, Resolution of the age structure of the detrital zircon populations of two Lower Cretaceous sandstones from the Weald of England by fission track dating: Geol. Mag., v. 14, p. 269–277.
Ilchik, R. P., 1990, Geology and geochemistry of the Vantage gold deposits, Alligator Ridge-Bald Mountain mining district, Nevada: ECON. GEOL., v. 85, p. 50–75.
Joralemon, P., 1951, The occurrence of gold at the Getchell mine, Nevada: ECON. GEOL., v. 46, p. 267–310.
Kistler, R. W., and Peterman, Z. E., 1978, Reconstruction of crustal blocks of California on the basis of initial strontium isotopic compositions of Mesozoic granitic rocks: U. S. Geol. Survey Prof. Paper 1071, p. 1–17.
Kornze, L. D., 1984, Geology of the Mercur gold mine: Utah Geol. Assoc. Pub. 13, p. 201–214.
Kowallis, B. J., Heaton, J. S., and Bringhurst, K., 1986, Fission-track dating of volcanically derived sedimentary rocks: Geology, v. 14, p. 19–22.
Kuehn, C. A., 1989, Studies of disseminated gold deposits near Carlin, Nevada: Evidence for a deep geologic setting of ore formation: Unpub. Ph.D. thesis, College Station, Pennsylvania State Univ., 395 p.
Lawrence, R. D., 1976, Strike-slip faulting terminates the Basin and Range province in Oregon: Geol. Soc. America Bull., v. 87, p. 846–850.
Levy, M., and Christie-Blick, N., 1989, Pre-Mesozoic palinspastic reconstruction of the eastern Great Basin (western United States): Science, v. 245, p. 1454–1462.
Mabey, D. R., Zietz, I., Eaton, G. P., and Kleinkopf, M. D., 1978, Regional magnetic patterns in part of the Cordillera in the western United States: Geol. Soc. America Mem. 152, p. 93–106.
Madrid, R. J., and Bagby, W. C., 1986, Structural alignment of sediment-hosted gold deposits in north-central Nevada: An example of inherited fabrics [abs.]: Geol. Soc. America Abstracts with Programs, v. 18, p. 393.
McDougall, I., and Harrison, T. M., 1988, Geochronology and thermochronology by the $^{40}Ar/^{39}Ar$ method: New York, Oxford Univ. Press, 212 p.
McKee, E. H., and Noble, D. C., 1986, Tectonic and magmatic development of the Great Basin of western United States during late Cenozoic time: Modern Geology, v. 10, p. 39–50.
Morton, J. L., Silberman, M. L., Bonham, H. F., Garside, L. J., and Noble, D. C., 1977, K-Ar ages of volcanic rocks, plutonic rocks and ore deposits in Nevada and eastern California—determinations run under the USGS-NBMG cooperative program: Isochron/West, no. 20, p. 19–29.
Naeser, C. W., 1976, Fission track dating: U. S. Geol. Survey Open-File Rept. 76–190, 65 p.
—— 1979, Fission-track dating and geologic annealing of fission tracks, *in* Jäger, E., and Hunziker, J. C., eds., Lectures in isotope geology: New York, Springer-Verlag, p. 154–169.
Naeser, C. W., and Crowley, K. D., 1989, Age equation and statistics of fission-track dating: Geol. Soc. America Ann. Mtg., 101st, St. Louis, Missouri, Oct. 28–Nov. 1, 1989, Short Course Notes, Chap. 2, 18 p.
Osterberg, M. W., 1990, Geology and geochemistry of the Chimney Creek gold deposit, Humboldt County, Nevada: Unpub. Ph.D. thesis, Tucson, Univ. Arizona, 173 p.
Ostwald, W., 1900, Uber die vermeintliche Isomerie des roten und gelben Quecksilberoxyds und die Oberflachenspannung fester Korper: Zeitsch. Physikalische Chemie, Stochiometrie Vewandschaftslehre, v. 34, p. 495–503.
Percival, T. J., Bagby, W. C., and Radtke, A. S., 1988, Physical and chemical features of precious metal deposits hosted by sedimentary rocks in the western United States, *in* Schafer, R. W., Cooper, J. J., and Vikre, P. G., eds., Bulk mineable precious metal deposits of the western United States. Symposium proceedings: Reno, Geol. Soc. Nevada, p. 11–34.
Poole, F. G., Claypool, G. E., and Fouch, T. D., 1983, Major episodes of petroleum generation in part of the northern Great Basin: Geothermal Resources Council Spec. Rept. 13, p. 207–213.
Radtke, A. S., 1985, Geology of the Carlin gold deposit, Nevada: U. S. Geol. Survey Prof. Paper 1267, 124 p.
Roberts, R. J., 1960, Alinements of mining districts in north-central Nevada: U. S. Geol. Survey Prof. Paper 400-B, p. B17–B19.
Rota, J. C., and Hausen, D. M., 1991, Geology of the Gold Quarry mine: Ore Geology Rev., v. 6, p. 83–105.
Seedorff, E., 1991, Magmatism, extension, and ore deposits of Eocene to Holocene age in the Great Basin—mutual effects and preliminary proposed genetic relationships, *in* Raines, G. L., Lisle, R. E., Schafer, R. W., and Wilkinson, W. H., eds., Geology and ore deposits of the Great Basin: Reno, Geol. Soc. Nevada, p. 133–178.
Sharpless, S., and Albers, J., 1987, A compilation of ages of mineralization of metallic mineral deposits in the western conterminous cordillera as determined through 1985: U. S. Geol. Survey Open-File Rept. 87–165, 28 p.
Shawe, D. R., 1965, Strike-slip control of basin-range structure indicated by historical faults in western Nevada: Geol. Soc. America Bull., v. 76, p. 1361–1378.
Silberman, M. L., and McKee, E. H., 1971, K-Ar dates of granitic plutons in north-central Nevada: Isochron/West, no. 1, p. 15–32.
Silberman, M. L., Berger, B. R., and Koski, R. A., 1974, K-Ar age relations of granodiorite emplacement and tungsten and gold mineralization near the Getchell mine, Humboldt County, Nevada: ECON. GEOL., v. 69, p. 646–656.
Sillitoe, R. H., and Bonham, H. F., 1990, Sediment-hosted gold deposits: Distal products of magmatic-hydrothermal systems: Geology, v. 18, p. 157–161.
Solomon, G. C., and Taylor, H. P., 1989, Isotopic evidence for the origin of Mesozoic and Cenozoic granitic plutons in the northern Great Basin: Geology, v. 17, p. 591–594.
Speed, R. C., 1979, Collided Paleozoic microplate in the western United States: Jour. Geology, v. 87, p. 279–292.
Staudacher, T., Jessberger, E. K., Dorflinger, D., and Kiko, J., 1978, A refined ultrahigh-vacuum furnace for rare gas analysis: Jour. Physics: Sci. Instrumentation, v. 11, sec. E, p. 781–784.

Stewart, J. H., 1980, Geology of Nevada: Nevada Bur. Mines Geology Spec. Pub. 4, 136 p.
Stewart, J. H., and Carlson, J. E., 1978, Geologic map of Nevada: U. S. Geol. Survey, scale 1:500,000.
Tooker, E. W., 1985, Discussion of the disseminated gold ore occurrence model: U. S. Geol. Survey Bull. 1646, p. 107–150.
Wells, J. D., Stoiser, L. R., and Elliott, J. E., 1969, Geology and geochemistry of the Cortez gold deposit, Nevada: ECON. GEOL., v. 64, p. 526–537.
Wilson, P. N., and Parry, W. T., 1990, Mesozoic hydrothermal alteration associated with gold mineralization in the Mercur district, Utah: Geology, v. 18, p. 866–869.
Zartman, R. E., 1974, Lead isotopic provinces of the western United States and their geological significance: ECON. GEOL., v. 69, p. 792–805.
Zeitler, P. K., Johnson, N. M., Briggs, N. D., and Naeser, C. W., 1982, Uplift history of the NW Himalaya as recorded by fission-track ages on detrital Siwalik zircons [abs.]: Mesozoic and Cenozoic Geology Symposium, 60th Anniversary Mtg., Bedaike, Geol. Soc. China, Program, p. 109.
—— 1988, Uplift history of the NW Himalaya as recorded by fission-track ages on detrital Siwalik zircons, *in* Jiqing, H., ed., Proceedings of the symposium on Mesozoic and Cenozoic geology, China: Beijing, Geol. Pub. House, p. 481–494.
Zimmerman, C., Knutsen, G. C., and Christensen, O. D., 1987, Lower Paleozoic stratigraphy of the Carlin trend, northeast Nevada: Implications for the Antler orogeny [abs.]: Geol. Soc. America Abstracts with Programs, v. 19, p. 905–906.
Zoback, M. L., Anderson, R. E., and Thompson, G. A., 1981, Cainozoic evolution of the state of stress and style of tectonism of the Basin and Range province of the western United States: Royal Soc. [London] Philos. Trans., v. A300, p. 407–434.

APPENDIX

Sample Descriptions

Numbers in first set of parentheses are field sample numbers; if core, then drill hole and depth in feet. Number in second set of parentheses is assay value.

FTZ-2 (241/1840) (1.9 g/t). Highly altered Goldstrike stock, 1,820- to 50-ft depth. From intensely argillized zone where rock is essentially quartz-pyrite-kaolinite. Within main ore zone.

FTZ-3 (213/1750) (24 g/t). Highly altered Goldstrike stock, 1,730- to 1,750-ft depth. From above postore dike in high-grade zone. Alteration comprises intense kaolinitization, with rock essentially quartz-pyrite-kaolinite.

FTZ-4 (PIT SS) (2.2 g/t). From pit bench 5240, 12075 N, 12000 E coordinates. Sandy unit in Rodeo Creek Formation, just above one of the major limestone units. Fairly clean, porous sandstone.

GSD-1 (118/1609) (0.6 g/t). Preore igneous dike slightly below main mineralized zone. Sericite laths up to 100 μm in length in biotite sites, with finer grained sericite and quartz replacing feldspars and groundmass. Quartz phenocrysts generally resorbed but unrecrystallized.

GSD-2 (260/1400) (0.4 g/t). Thin, intensely sericitized and fluidized breccia dike, probably equivalent in age to the postore dike. Contains fragments of mineralized sedimentary rock. The only evidence of former phenocrysts are booklets of sericite which are probably after biotite. Analyzed <2-μm fraction.

GSD-3 (BP-91) (7.9 g/t). Rock comprises sparse quartz eyes set in a sericite matrix. What were probably originally feldspar phenocrysts are represented by coarser grained sericite + kaolinite clots. Groundmass is a mass of fine-grained interlocking sericite and quartz. Sample has been subjected to intense weathering, thus pyrite is absent. Analyzed <2-μm fraction.

GSD-4 (1682/2109) (2.1 g/t). Intensely sericitized dike rock, with little of the original texture preserved. Some clots of slightly coarser sericite probably represent former feldspar phenocrysts. Of all the age samples from dikes, this contains the most pyrite (about 5%); detectable As is present in the pyrite, particularly near the rims. This sample also contained abundant kaolinite as replacement patches and in stringers. Analyzed <2-μm fraction.

GSD-5 (276/972) (3.4 g/t). Porphyritic-aphanitic dike completely converted to quartz-sericite-pyrite. Quartz phenocrysts have been completely recrystallized; no strong evidence is present for other mineral phases as phenocrysts, though some of the more coarsely crystalline sericite may represent former biotite. Analyzed <2-μm fraction.

GSS-1 (ST7/975). Fresh Goldstrike stock; medium-grained equigranular monzonite containing biotite, hornblende, plagioclase, and orthoclase with minor amounts of quartz and pyroxene.

GSS-2 (ST7/2383). Fresh Goldstrike stock, similar to ST7/975 but with slightly more quartz and orthoclase.

GSS-3 (208/1661) (48 g/t). High-grade ore from within the Goldstrike stock. The material analyzed comprised a <2-μm separate of hydrothermal sericite replacing the rock groundmass and feldspar sites. A few individual sericite laths were up to 100 μm in length, but these were of insufficient quantity and such poor constitution that separation for stepheating was impossible.

MCC-3. Typical Roberts Mountains Formation laminated silty limestone, comprising roughly 20 to 40 percent detrital grains set in a carbonate matrix (from Maggie Creek Canyon, 25 km southeast of Post-Betze). Trace amounts of feldspar, zircon, apatite, and muscovite are present as part of the detrital component. Diagenetic pyrite comprises less than 1 percent of the rock, and only traces of organic matter are present. Analyzed <2-μm fraction.

POD-1 (213/1780). Postore dike from near core of ore zone. Rock comprises sparse biotite and feldspar phenocrysts set in aphanitic matrix. Biotite appears fresh in thin section but feldspars are weakly to moderately sericitized.

SED-2 (230/1567) (5.8 g/t). Extremely porous, decarbonatized Roberts Mountains Formation, comprising dominantly detrital quartz with minor diagenetic and hydrothermal pyrite. Silicification takes the form of irregular veinlets, stringers, and patches and comprises between 30 and 60 percent of the rock. Hydrothermal sericite is closely associated spatially with silification; in excess of 90 percent of the K-bearing mica in the rock in thin section is in silicified areas or fractures cutting silicified patches. Texturally, sericite is cogenetic with, or slightly younger than, hydrothermal gold-bearing arsenian pyrite and arsenopyrite. No mica of obvious detrital or diagenetic origin was observed in thin section.

SED-3 (3/1537) (0.2 g/t). Medium gray, decarbonatized rock from the Roberts Mountains Formation below the main ore zone composed of predominantly quartz grains (50–80%) in what was formerly a matrix of carbonate (now open space). Original bedding is quite distinct in most of the core. Detrital muscovite comprises an estimated 0.1 percent of the rock, which is abundant relative to most samples of Roberts Mountains Formation. Locally, black organic matter may constitute up to 2 percent of the rock; cubic diagenetic pyrite makes up approximately 1 percent of the rock; no arsenic-bearing (ore-stage) pyrite was observed in this sample. The muscovite and organic matter show structures in a few places, which suggests a volume decrease and concomitant reorientation of micas may have taken place; this volume decrease is most likely due to decarbonatization and later faulting.

SED-4 (1682/2452) (0.1 g/t). Highly sheared sedimentary rock with much introduced sericite (on a local scale). Contains pods and patches of strained carbonate and a few irregular thin stringers of calcite. Moderately bleached of any organic component. From adjacent to Goldstrike stock, within <200 m of contact. Analyzed <2-μm fraction.